

ELECTRONIC SUPPLEMENTARY INFORMATION

for

Ruthenium Catalyst linked to a Redox-Active Ruthenium Polypyridine for
Water Oxidation

Fernando F. Salomon,^{a,b} Pedro O. Abate,^{a,b} and Luis M. Baraldo^{a,b*}

^a Universidad de Buenos Aires, Facultad de Ciencias Exactas y Naturales, Departamento de Química Inorgánica, Analítica y Química Física, Pabellón 2, Ciudad Universitaria, C1428EHA, Buenos Aires, Argentina.

^b CONICET – Universidad de Buenos Aires. Instituto de Química Física de Materiales, Medio Ambiente y Energía (INQUIMAE), Pabellón 2, Ciudad Universitaria, C1428EHA, Buenos Aires, Argentina.

Table of contents

<i>Figure S1</i>	3	<i>Table S10</i>	31
<i>Figure S2</i>	4	<i>Figure S34.</i>	32
<i>Figure S3</i>	4	<i>Table S11</i>	32
<i>Figure S4</i>	5	<i>Figure S35.</i>	33
<i>Figure S5</i>	6	<i>Table S12</i>	33
<i>Figure S6</i>	7	<i>Figure S36.</i>	34
<i>Figure S7</i>	8	<i>Table S13</i>	34
<i>Figure S8</i>	9	<i>Figure S37.</i>	35
<i>Figure S9</i>	10	<i>Table S14</i>	35
<i>Figure S10</i>	10	<i>Figure S38.</i>	36
<i>Figure S11</i>	11	<i>Table S15</i>	36
<i>Figure S12</i>	12	<i>Table S16</i>	37
<i>Figure S13</i>	13	<i>Figure S39.</i>	38
<i>Figure S14</i>	13	<i>Table S17</i>	38
<i>Figure S15.</i>	14	<i>Figure S40.</i>	39
<i>Figure S16.</i>	14	<i>Table S18</i>	39
<i>Figure S17.</i>	15	<i>Table S19</i>	40
<i>Figure S18.</i>	16	<i>Figure S41.</i>	41
<i>Figure S19.</i>	16	<i>Table S20</i>	41
<i>Figure S20.</i>	17	<i>Figure S42.</i>	42
<i>Figure S21.</i>	17	<i>Table S21</i>	42
<i>Figure S22.</i>	18	<i>Table S22</i>	43
<i>Figure S23.</i>	18	<i>Figure S43.</i>	44
<i>Figure S24.</i>	19	<i>Table S23</i>	44
<i>Figure S25.</i>	20	<i>Figure S44.</i>	45
<i>Figure S26.</i>	21	<i>Table S24</i>	45
<i>Scheme S1</i>	21	<i>Table S25</i>	46
<i>Table S1</i>	21	<i>Figure S45.</i>	47
<i>Figure S27.</i>	22	<i>Table S26</i>	47
<i>Table S2.</i>	22	<i>Figure S46.</i>	48
<i>Figure S28.</i>	23		
<i>Table S3.</i>	24		
<i>Figure S29.</i>	25		
<i>Table S4.</i>	25		
<i>Figure S30.</i>	26		
<i>Table S5.</i>	26		
<i>Table S6.</i>	27		
<i>Figure S31.</i>	28		
<i>Table S7.</i>	28		
<i>Figure S32.</i>	29		
<i>Table S8.</i>	29		
<i>Table S9.</i>	30		
<i>Figure S33.</i>	31		

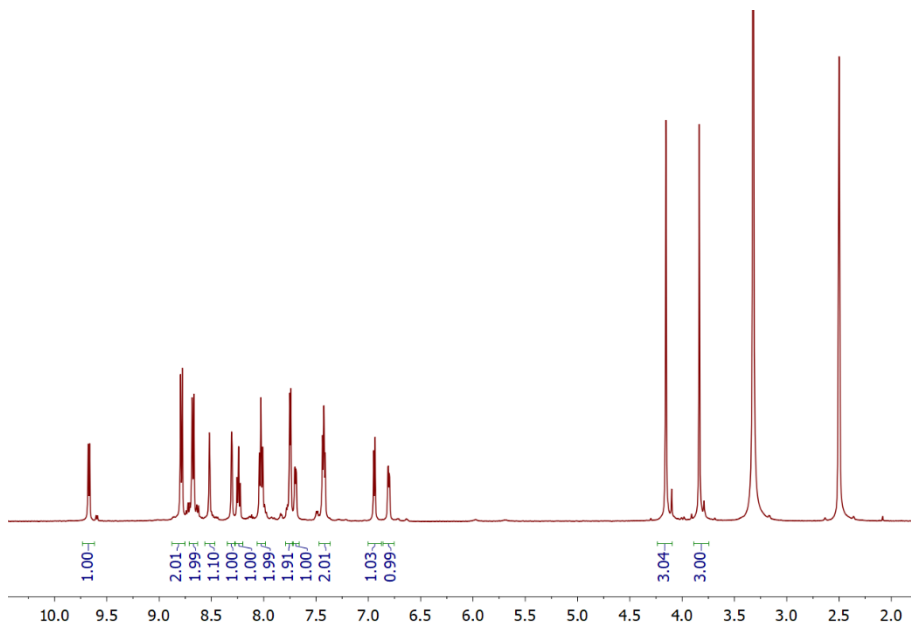
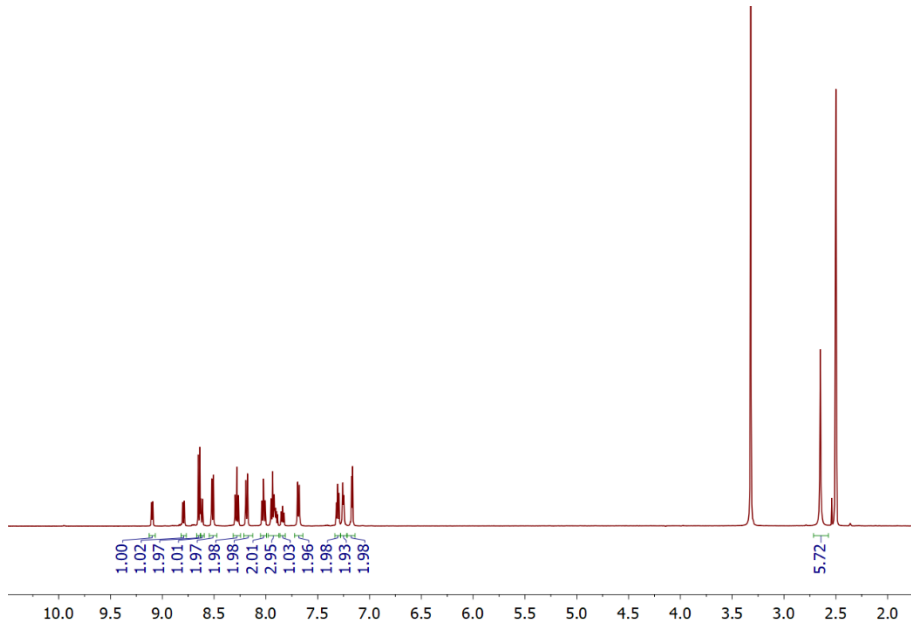


Figure S1. 500 MHz ^1H -NMR spectrum of $[\text{Ru}(\text{tpy})(\text{MeO}-\text{bpy})\text{CN}](\text{PF}_6)$ dissolved in d_6 -DMSO.



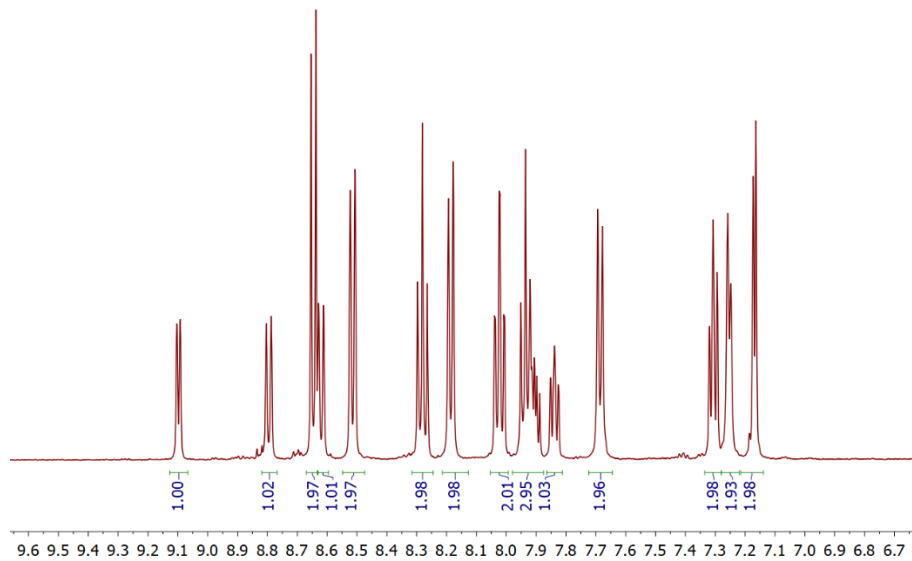


Figure S2. 500 MHz ^1H -NMR spectrum of **(1)** dissolved in d_6 -DMSO. (top) Full scale. (bottom) Aromatic region.

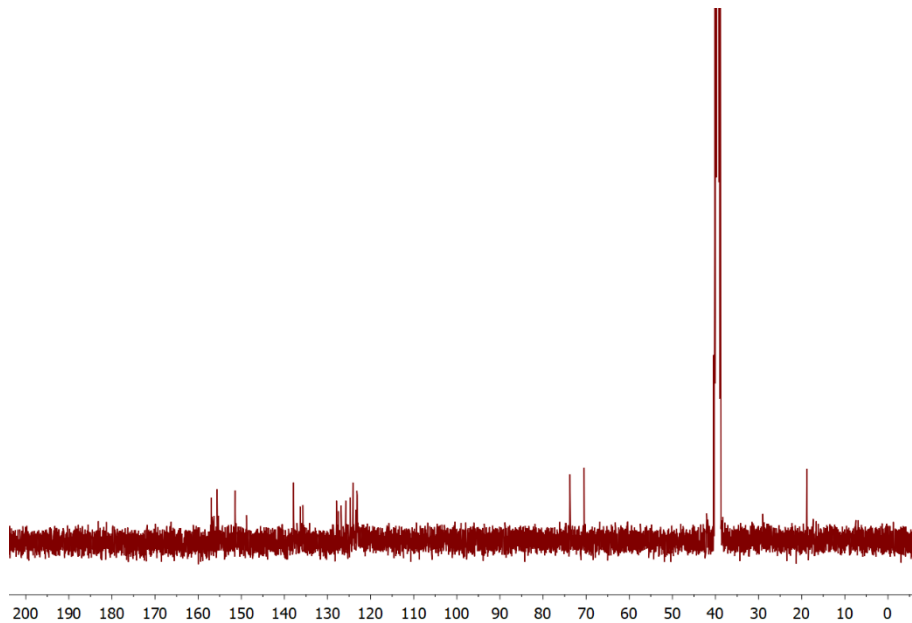


Figure S3. 125 MHz ^{13}C -NMR spectrum of **(1)** dissolved in d_6 -DMSO.

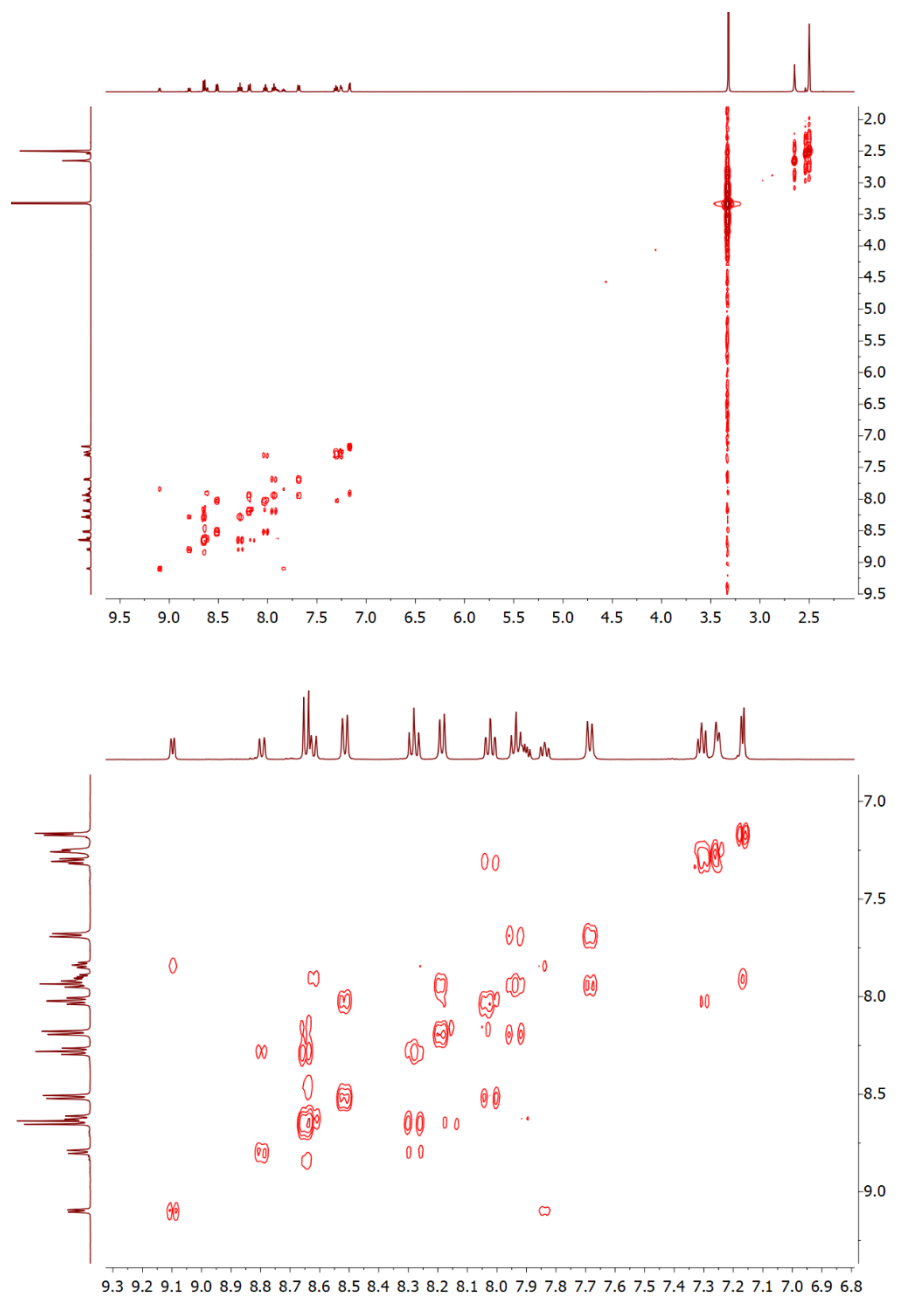


Figure S4. 2D ^1H - ^1H COSY spectrum of (**1**) dissolved in d_6 -DMSO. (top) Full scale. (bottom) Aromatic region.

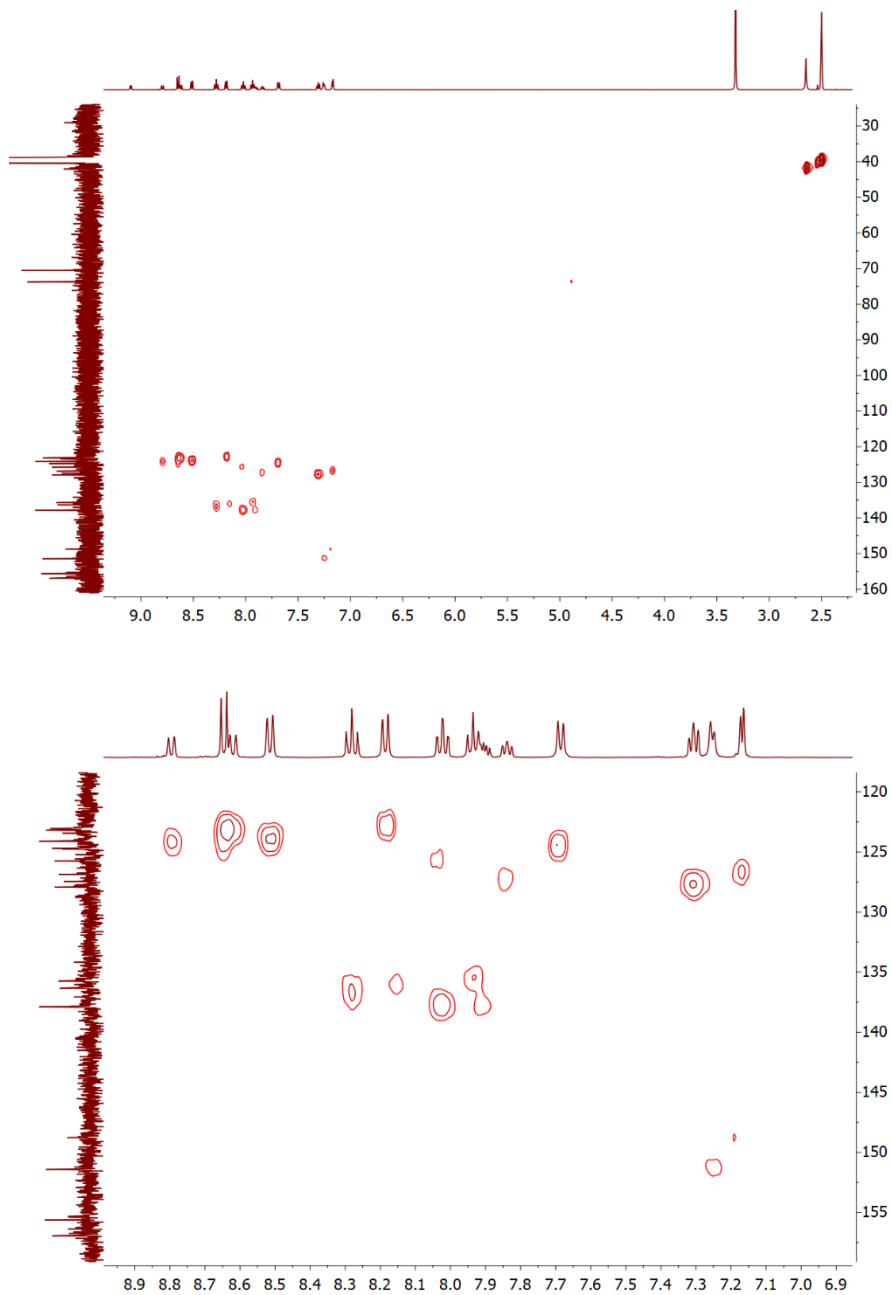


Figure S5. 2D ^1H - ^{13}C HSQC spectrum of **(1)** dissolved in d_6 -DMSO. (top) Full scale. (bottom) Aromatic region.

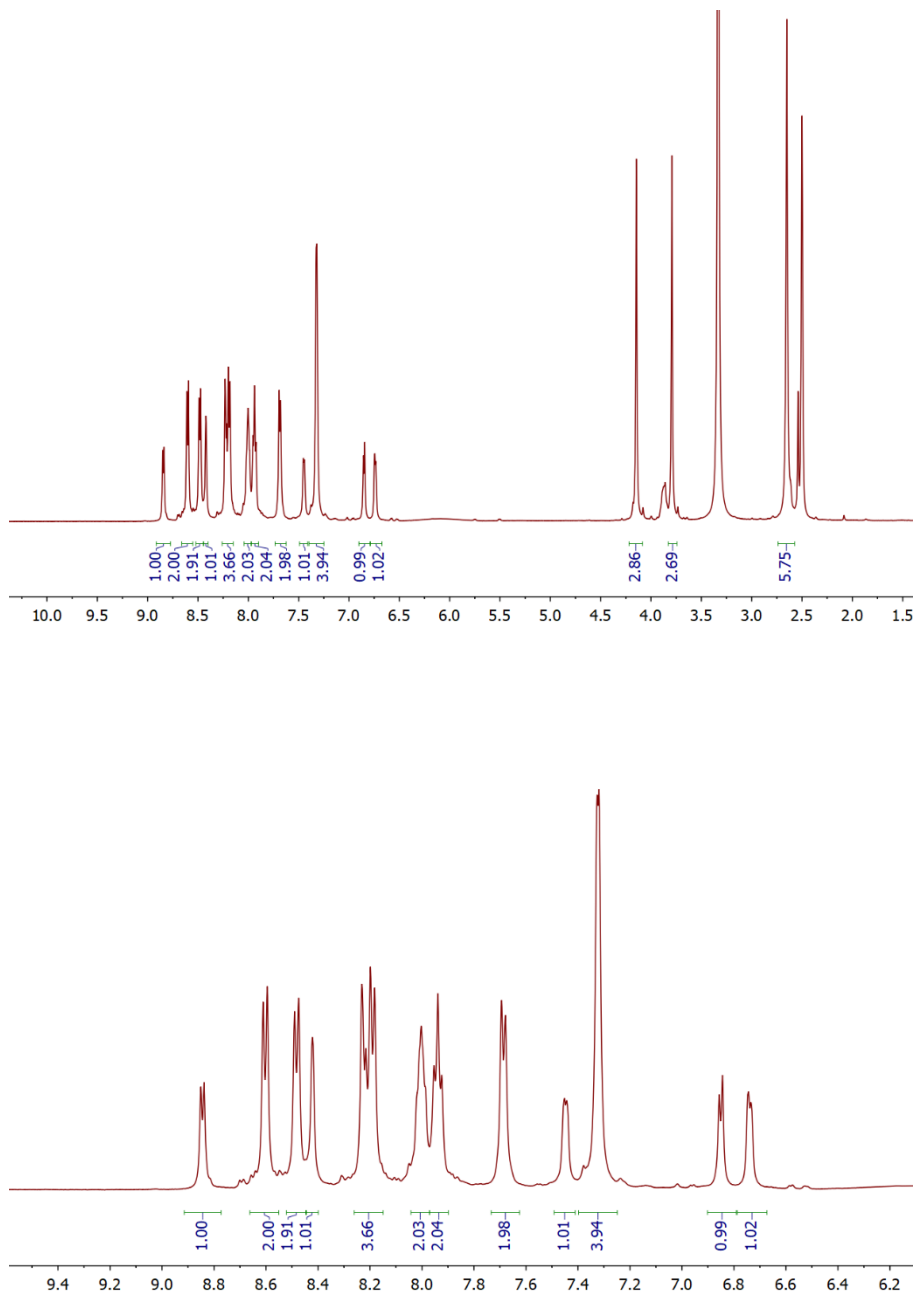


Figure S6. 500 MHz ^1H -NMR spectrum of (**2**) dissolved in d_6 -DMSO. (top) Full scale. (bottom) Aromatic region.

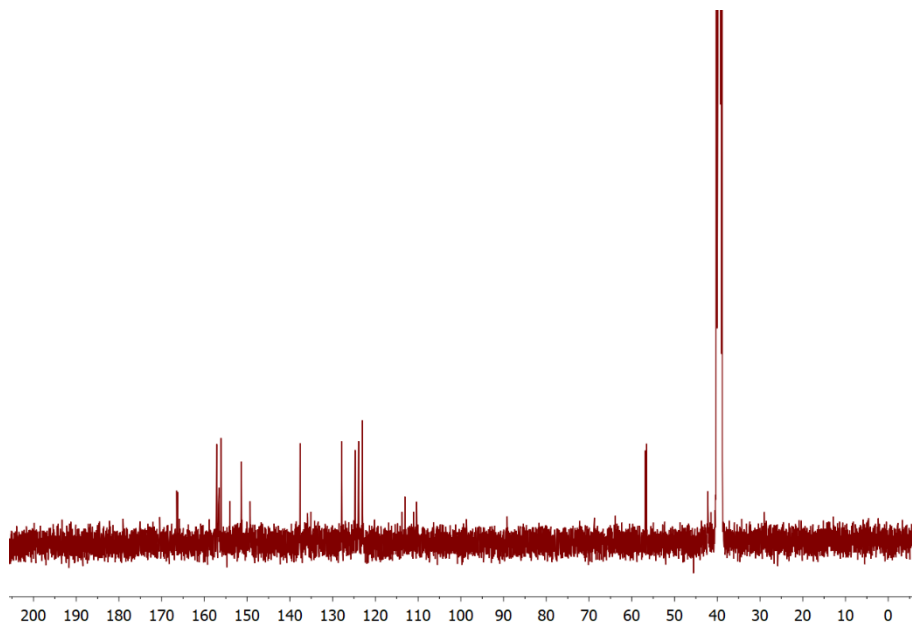
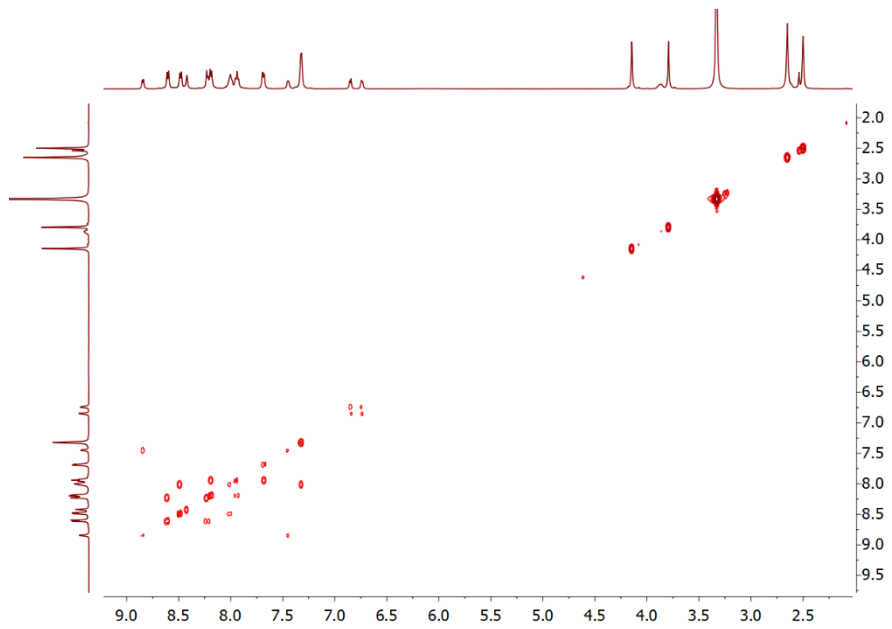


Figure S7. 125 MHz ^{13}C -NMR spectrum of (2) dissolved in d_6 -DMSO.



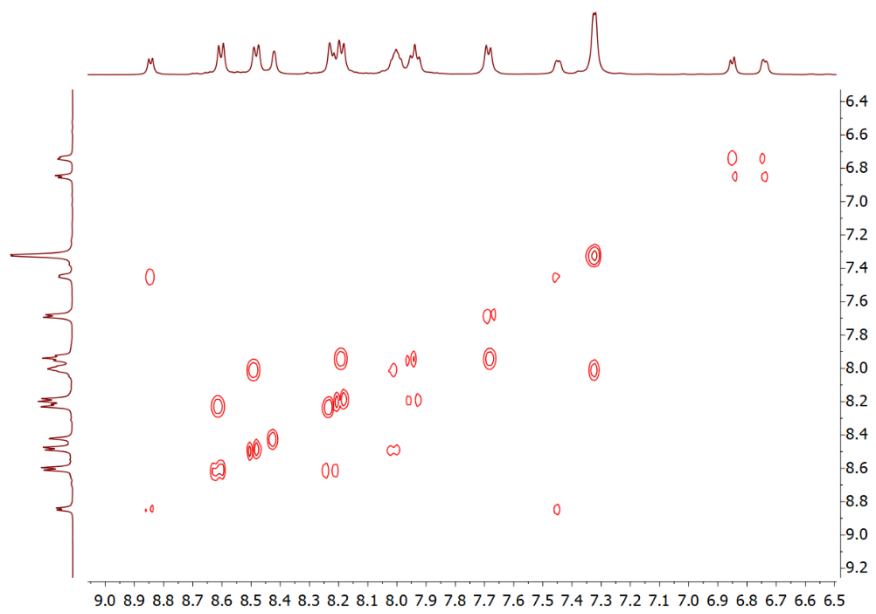
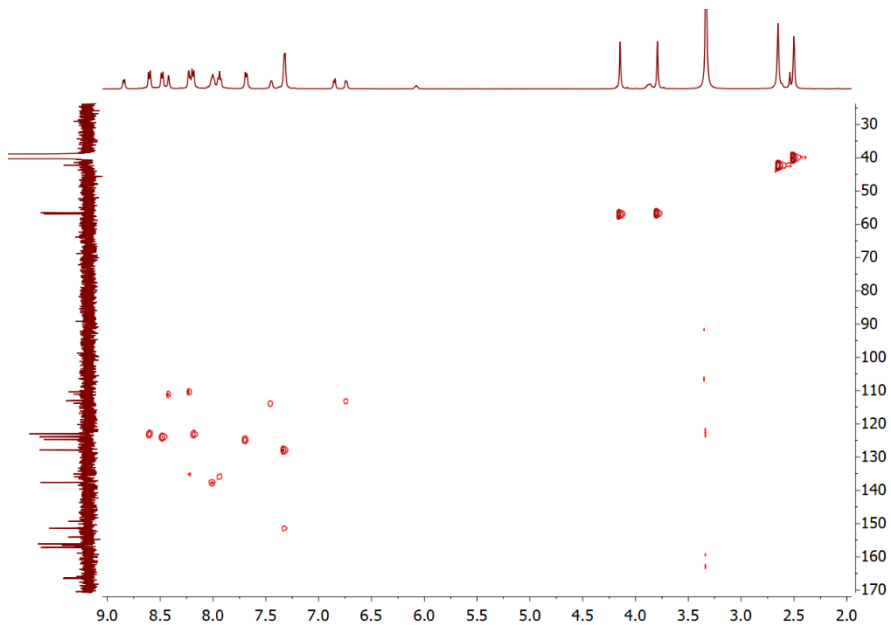


Figure S8. 2D ^1H - ^1H COSY spectrum of (2) dissolved in d_6 -DMSO. (top) Full scale. (bottom) Aromatic region.



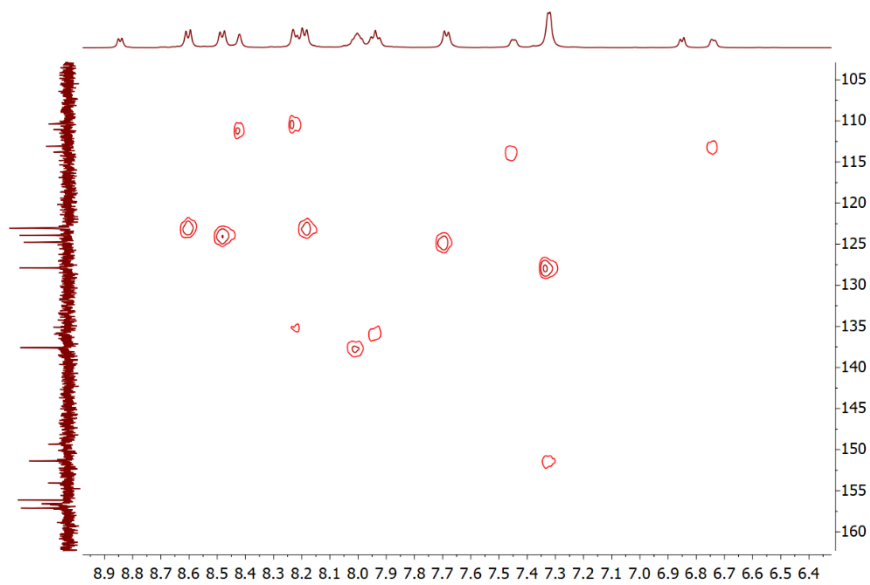


Figure S9. 2D ^1H - ^{13}C HSQC spectrum of (2) dissolved in d_6 -DMSO. (top) Full scale. (bottom) Aromatic region.

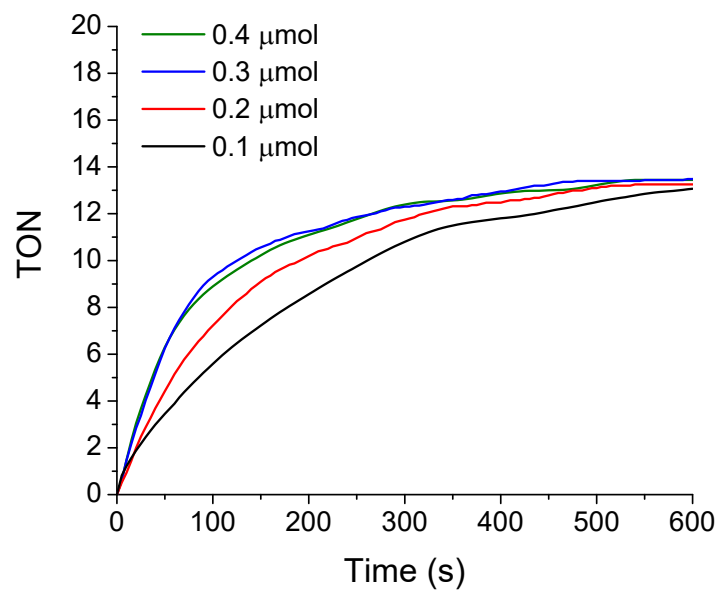


Figure S10. O_2 concentration detected using a Clark electrode vs. time at different concentrations of (1) in 0.1M triflic acid ($\text{pH} = 1$) with $[\text{Ce(IV)}] = 0.21 \text{ M}$ as oxidant.

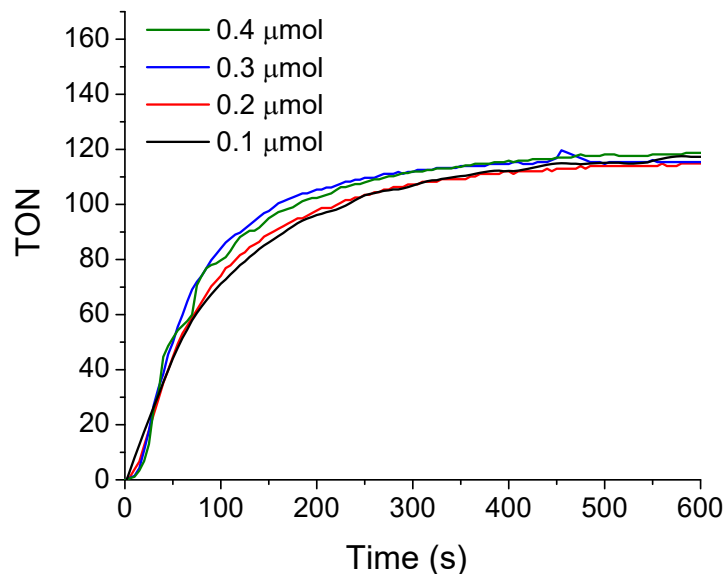
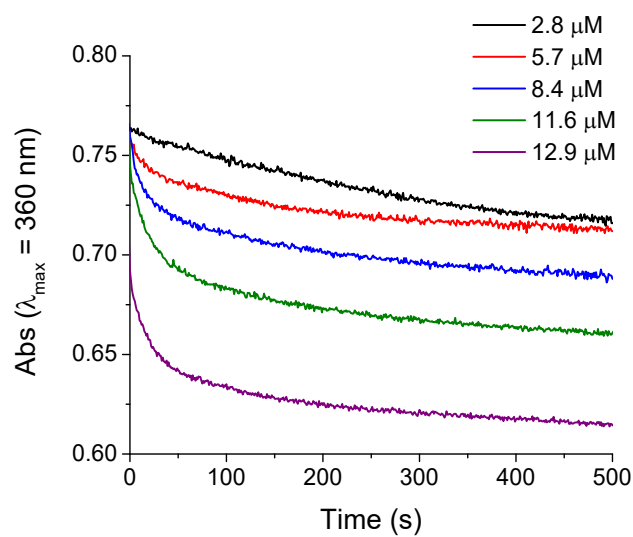


Figure S11. O_2 concentration detected using a Clark electrode vs. time at different concentrations of (**2**) in 0.1M triflic acid ($pH = 1$) with $[Ce(IV)] = 0.28\text{ M}$ as sacrificial oxidant.



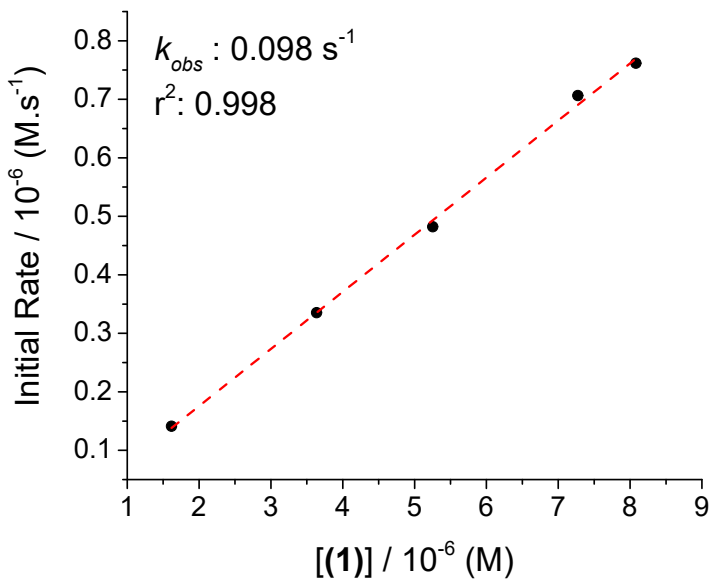
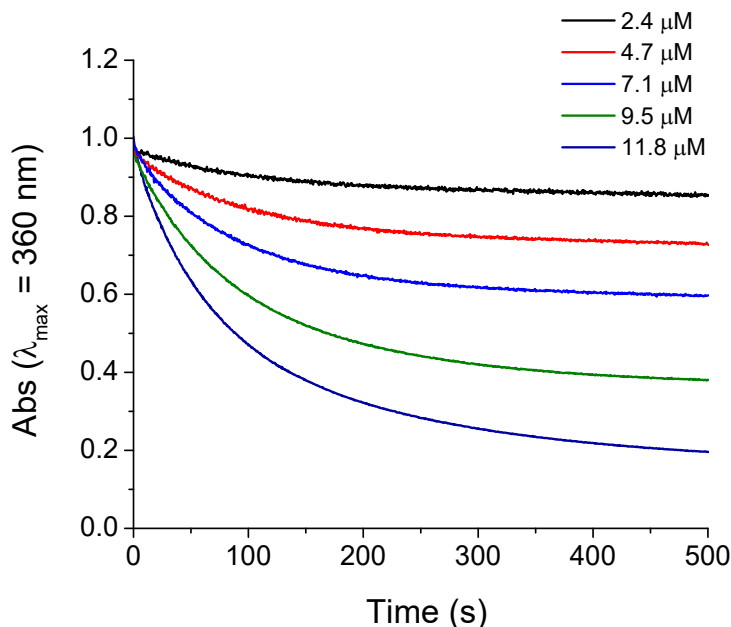


Figure S12. (Top) Absorbance decay monitored at 360 nm in aqueous solution as a function of time for different concentrations of (1). (Bottom) Plot of the rate constant vs concentrations of (1). Conditions: $[Ce(IV)] = 1.78\text{ mM}$, $pH = 1.0$ (aqueous 0.1 M triflic acid) and $T = 298\text{ K}$.



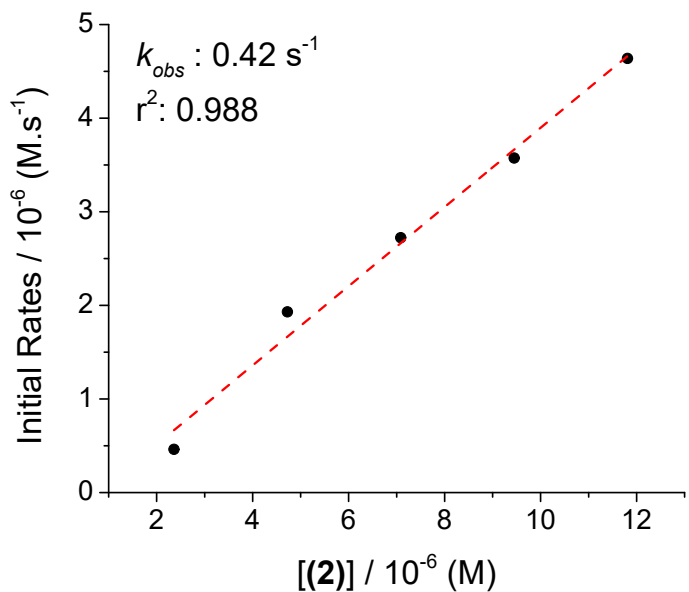


Figure S13. (Top) Absorbance decay monitored at 360 nm in aqueous solution as a function of time for different concentrations of (2). (Middle) Plot of the rate constant vs concentrations of (2). Conditions: [Ce(IV)] = 2.89 mM, pH = 1.0 (aqueous 0.1 M triflic acid) and T = 298 K.

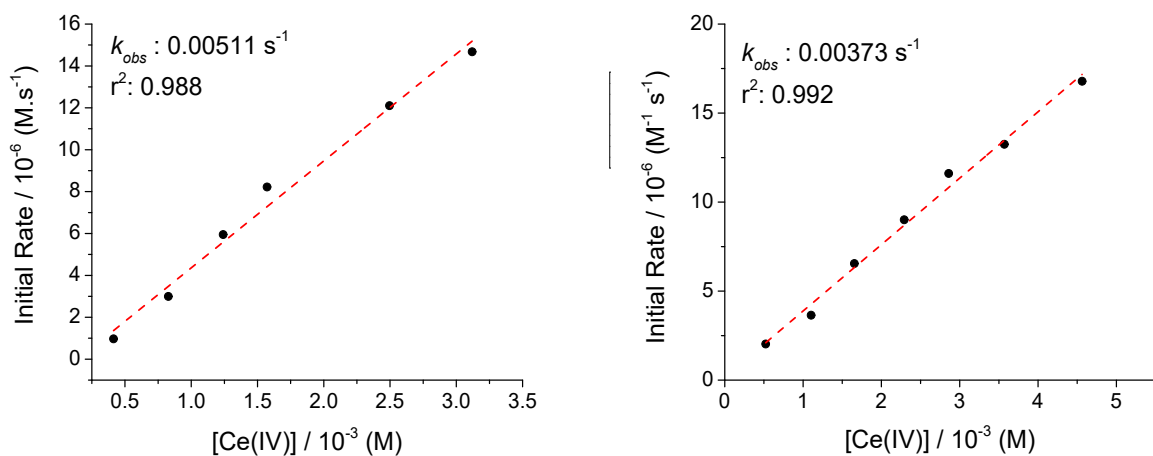


Figure S14. Plot of the rate constant vs concentrations of [Ce(IV)] for (1) (Left) and (2) (Right). Conditions: [(1)] = 35.6 μ M, [(2)] = 37.5 μ M, pH = 1.0 (aqueous 0.1 M triflic acid) and T = 298 K.

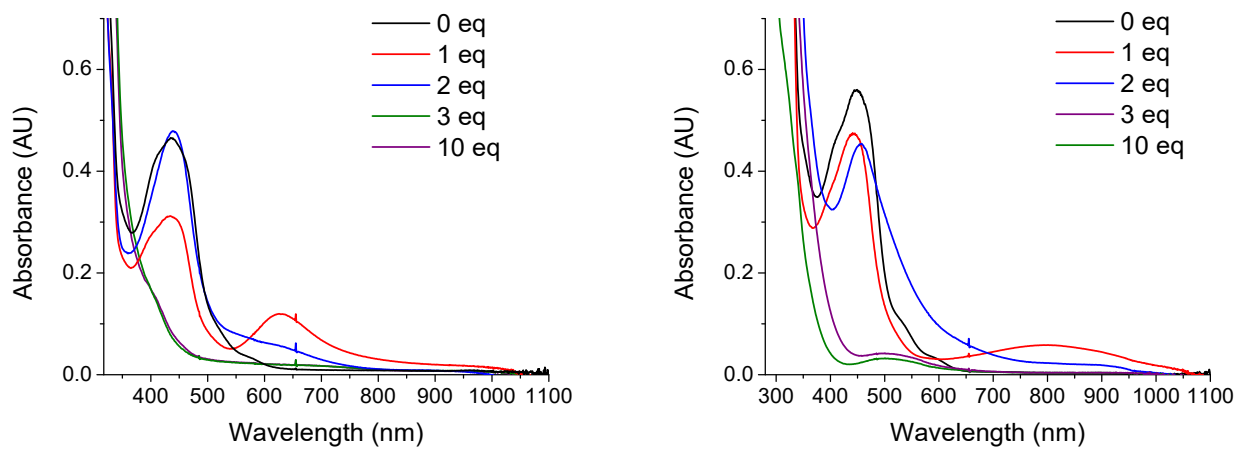


Figure S15. UV-vis spectra for **(1)** (Left) and **(2)** (Right) after the addition of 1, 2, 3 and, 10 eq. of Ce(IV) in 0.1M triflic acid ($pH = 1$).

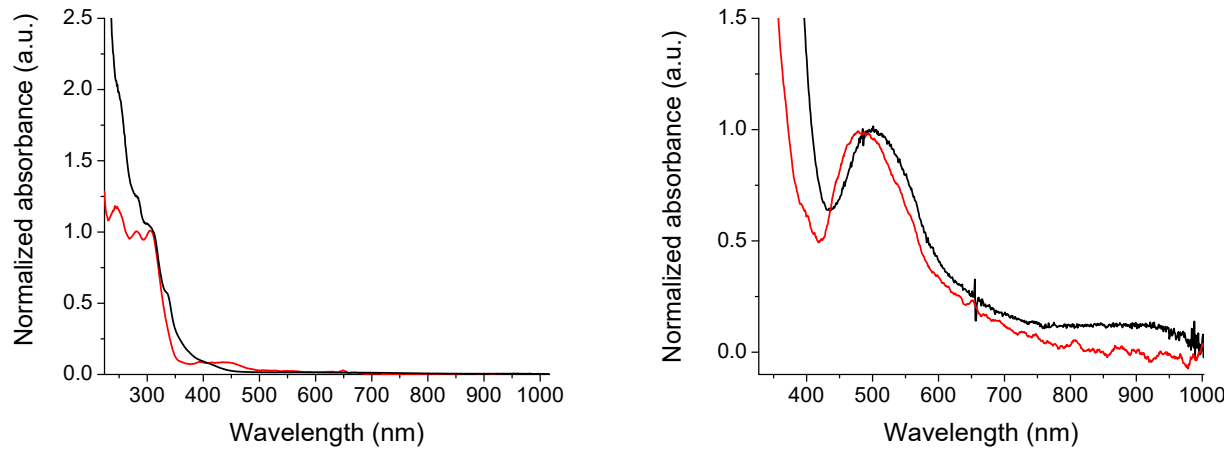


Figure S16. Normalized UV-vis spectra of **(1)** (Left) and **(2)** (Right) in the resting state after addition of 240 eq. of Ce(IV) in 0.1M triflic acid ($pH = 1$) (red trace) and after a three-electron oxidation process in a spectroelectrochemistry experiment.

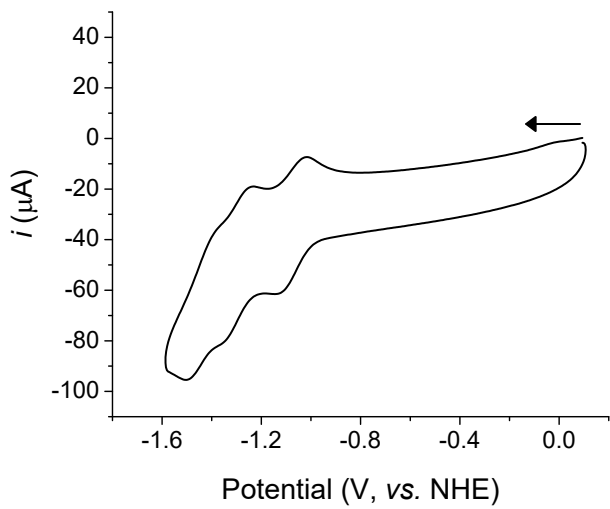
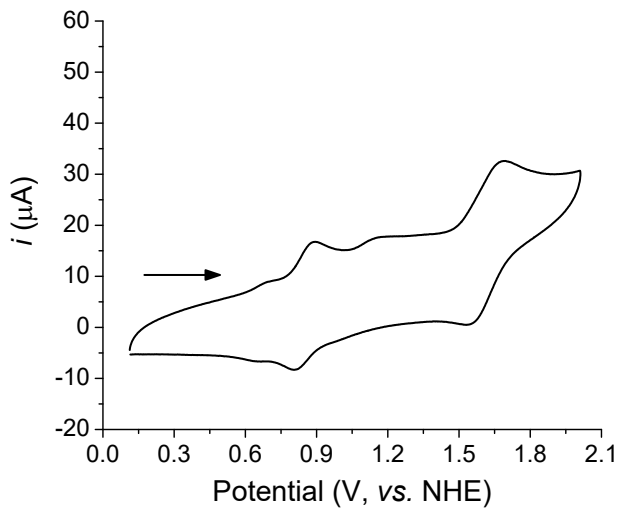


Figure S17. **(Top)** Anodic and **(Bottom)** cathodic cyclic voltammogram of **(2)** in propylene carbonate / 0.1M tetrabutylammonium hexafluorophosphate. ($[2] = 3\text{mM}$; $v = 0.1 \text{ V.s}^{-1}$).

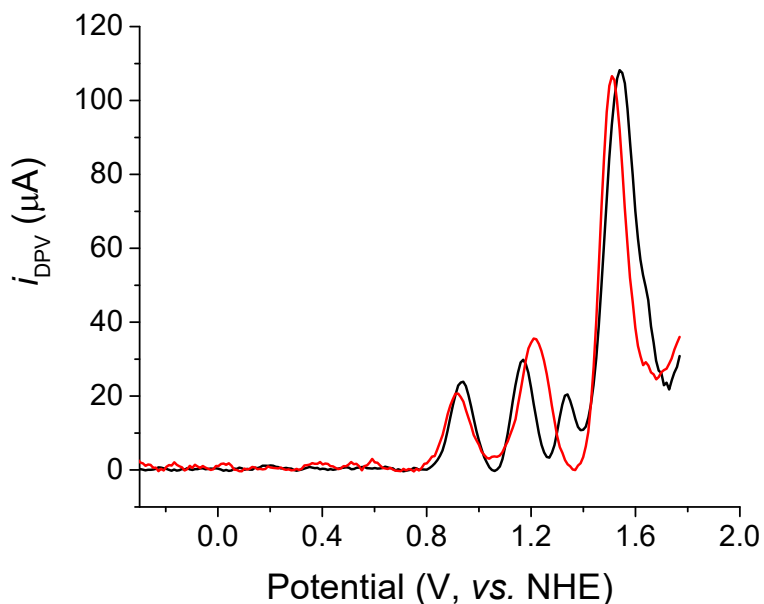


Figure S18. Differential pulse voltammetry experiment of (1) (black trace) and (2) (red trace) in 0.1 M trifluoromethanesulfonic acid ($pH = 1.0$). Conditions: WE: glassy carbon electrode, CE: platinum coil, RE: Ag/AgCl 3M NaCl, $[1] = 2.0 \text{ mM}$ and, $[2] = 2.0 \text{ mM}$. For (2), 7% propylene carbonate as co-solvent.

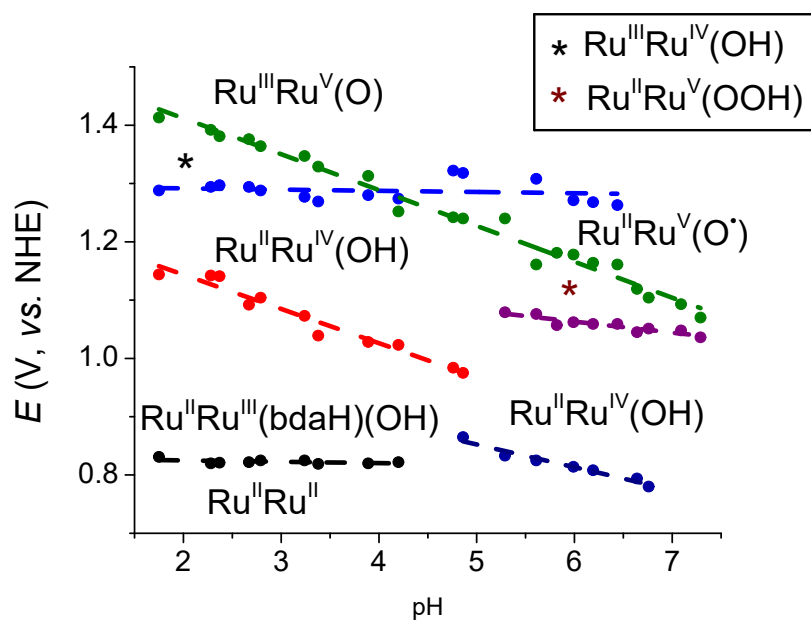


Figure S19. Potential vs pH diagram for (2) in aqueous phosphate buffer. Conditions: WE: glassy carbon electrode, CE: platinum coil, RE: Ag/AgCl 3M NaCl.

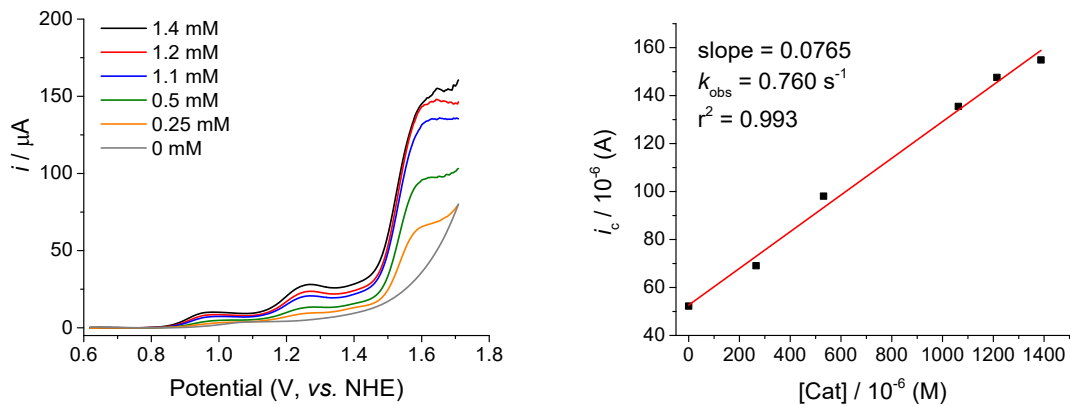


Figure S20. (Left) Linear Sweep Voltammetry of (2) at $v = 50 \text{ mV.s}^{-1}$ in 0.1 M trifluoromethanesulfonic acid ($\text{pH} = 1.0$) for different catalyst concentrations. (Right) Variation of the catalytic current vs catalyst concentration.

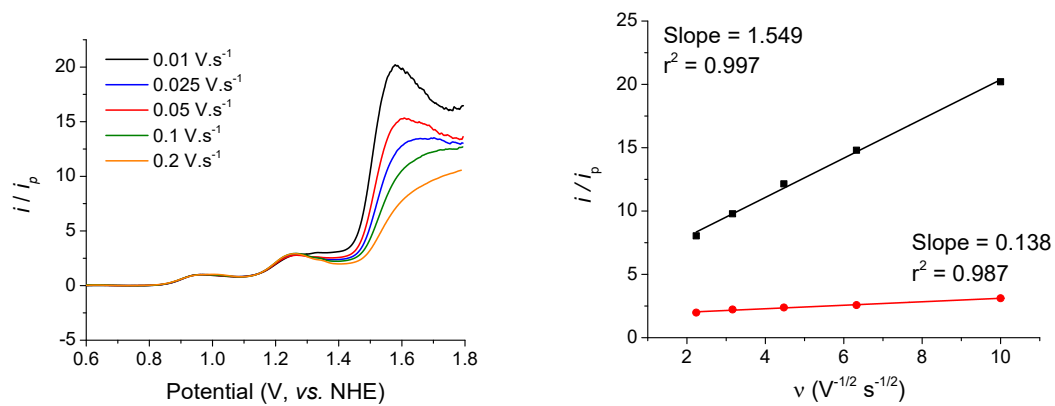
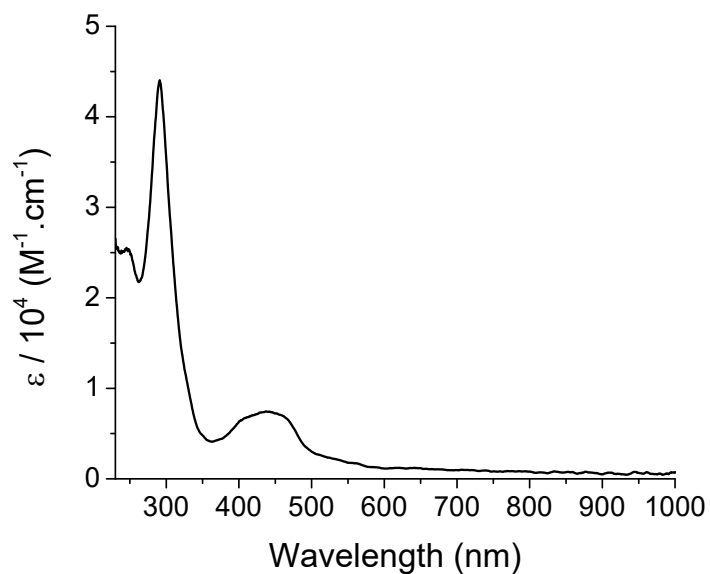


Figure S21. (Left) Linear Sweep Voltammetry of (2) in 0.1 M triflic acid ($\text{pH} = 1$) at different scan rates normalized by the peak current for the first oxidation process. (Right) Plot of normalized current (i / i_p) measured at 1.6 V (black trace) and 1.4 V (red trace) vs. squared root of scan velocity. Conditions: WE (glassy carbon electrode), CE (platinum wire), RE (Ag/AgCl 3 M NaCl).



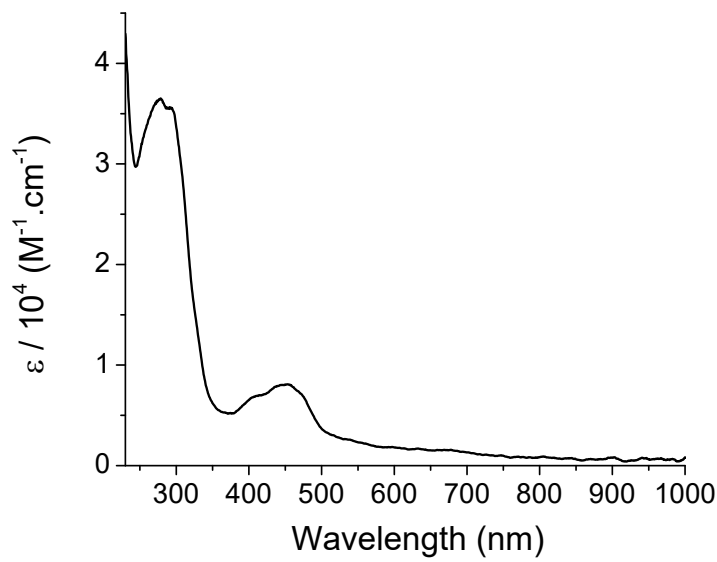


Figure S22. UV-vis spectrum of (1) (Top) and (2) (Bottom) in 0.1M triflic acid ($\text{pH} = 1$).

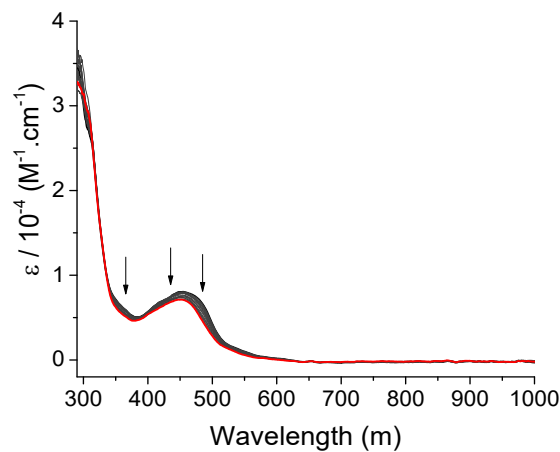


Figure S23. Spectroelectrochemistry experiments of (2) in 0.1M tetrabutylammonium hexafluorophosphate in propylene carbonate solution.

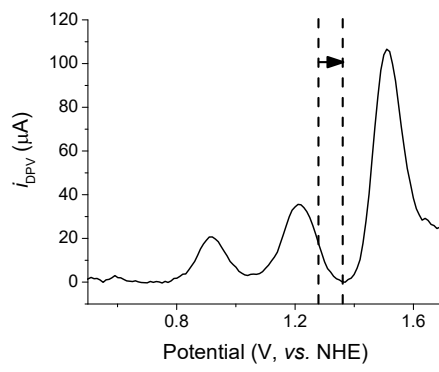
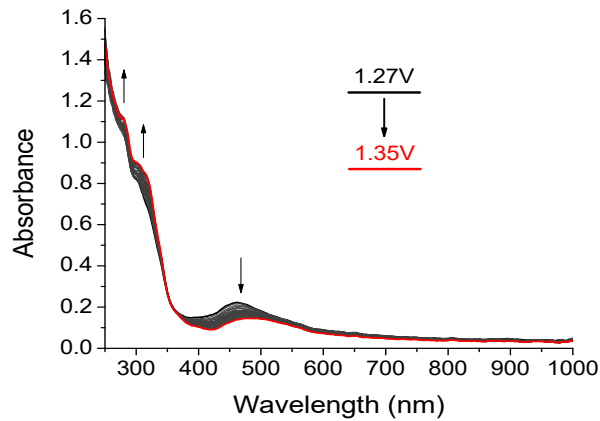
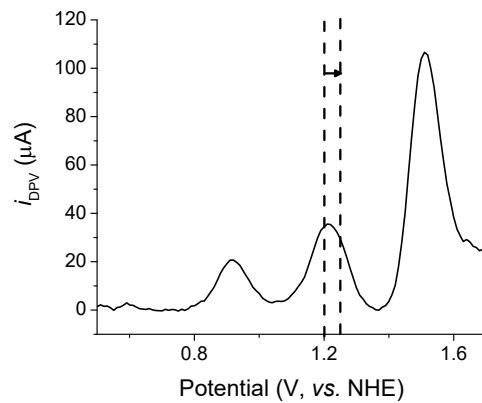
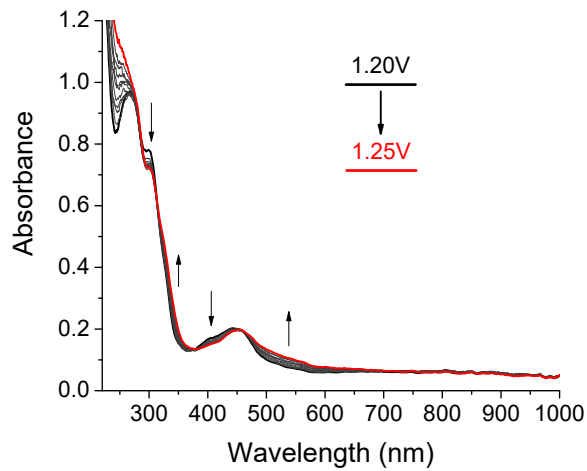
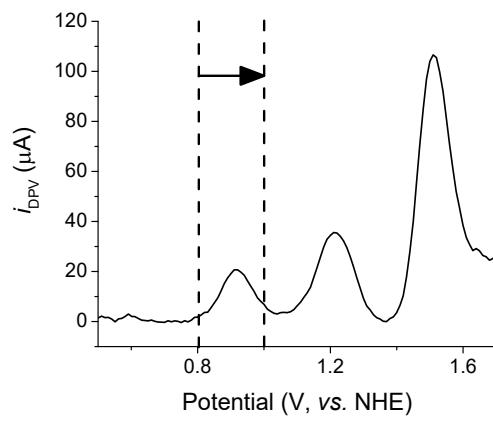
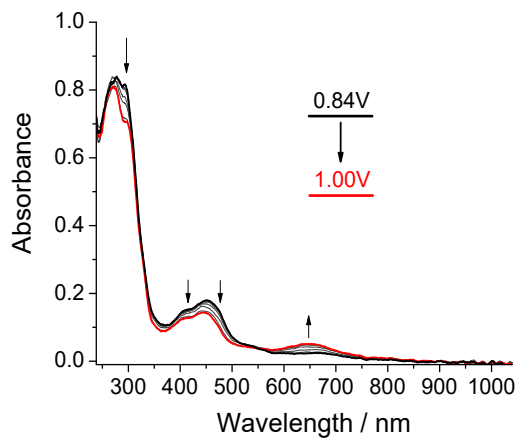


Figure S24. Spectroelectrochemistry of (2) in 0.1 M trifluoromethanesulfonic acid ($\text{pH} = 1$) for the first three oxidation processes. The arrows indicate changes during the different oxidation process. Conditions: WE: Pt, CE: Pt, RE: Ag/AgCl 3M NaCl.

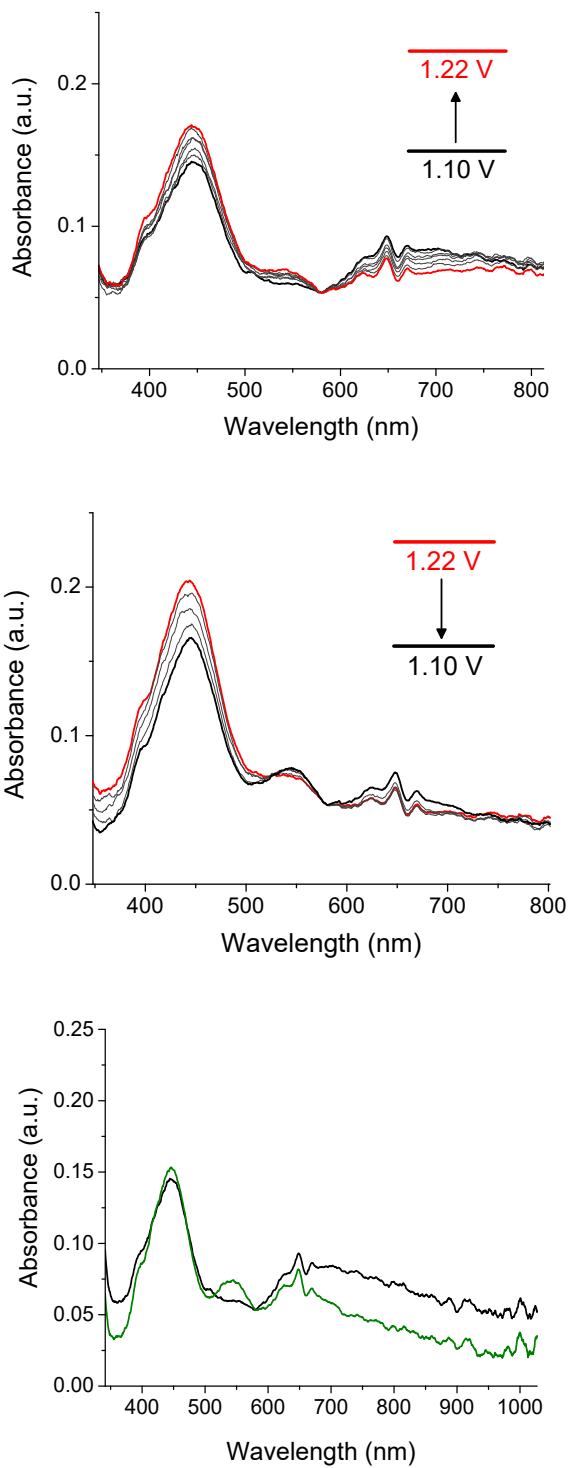


Figure S25. Spectroelectrochemistry experiments of (**1**) in 0.1M triflic acid ($\text{pH} = 1$) sweeping back and forth between 1.10V and 1.22V. (Top) UV-vis spectra collected while changing the applied potential from 1.10V to 1.22V. (Middle) UV-vis spectra collected while changing the applied potential from 1.22V to 1.10V. (Bottom) Comparison between the UV-vis spectra at $E=1.10$ V before (black trace) and after (green trace) the experiment.

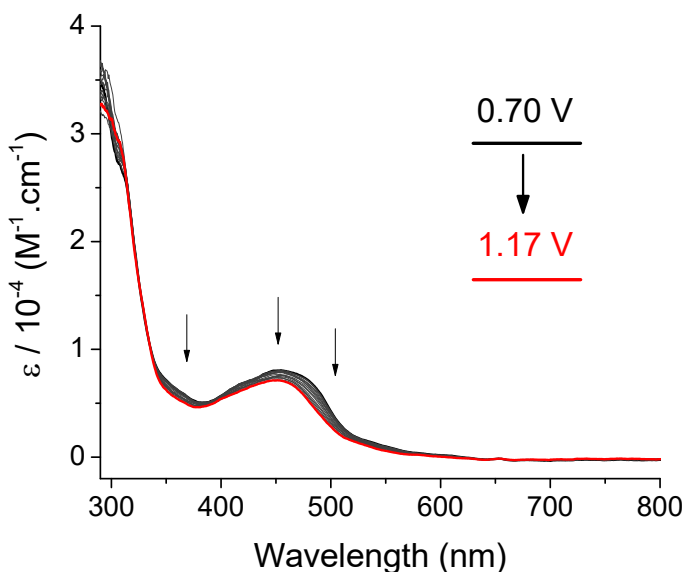
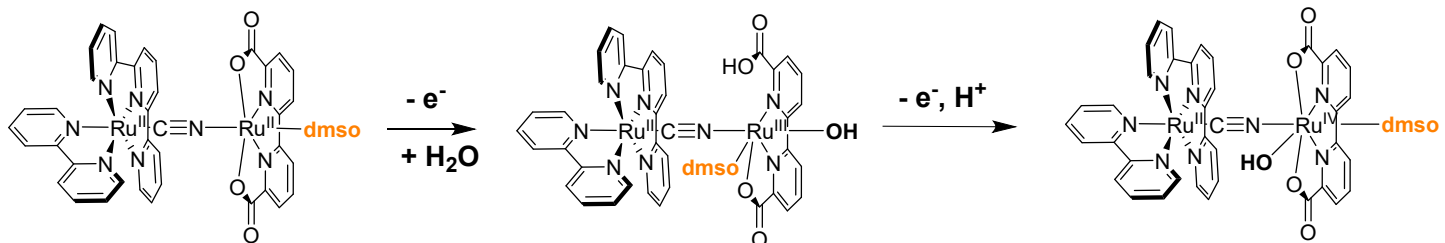


Figure S26. Spectroelectrochemistry experiments of (1) in 0.1M tetrabutylammonium hexafluorophosphate in propylene carbonate solution.



Scheme 1. Oxidation steps proposed for the studied complexes including the isomerization in the $\text{Ru}^{\text{II}}\text{-CN-Ru}^{\text{III}}\text{-OH}_2$ specie.

Table S1. Energies values and percentual group contributions of selected MO's of complex $[\text{Ru}^{\text{II}}(\text{bpy})\text{-Ru}^{\text{II}}(\text{bda})]^+$ in their singlet ground state.

MO's	Energy (eV)	Ru_{bda}	bda	DMSO	CN	Ru_{tpy}	tpy	bpy
L+10	-0,82	41	8	18	7	4	20	1
L+9	-1,47	0	0	0	0	4	67	29
L+8	-1,48	0	0	0	0	1	2	97
L+7	-1,58	0	0	0	0	1	99	0
L+6	-1,72	0	0	0	0	1	29	70
L+5	-1,88	4	95	0	0	0	0	0
L+4	-2,22	1	98	1	0	0	0	0
L+3	-2,51	0	0	0	0	4	59	36
L+2	-2,56	3	37	1	0	1	26	32
L+1	-2,57	5	52	1	0	1	14	27
LUMO	-2,71	0	1	0	1	6	91	1
HOMO	-5,16	70	27	0	1	1	0	0

H-1	-5,62	50	20	1	6	18	3	1
H-2	-5,77	51	16	2	7	19	4	1
H-3	-6,08	2	1	0	0	76	8	11
H-4	-6,22	12	10	0	4	54	14	6
H-5	-6,4	18	9	0	5	53	14	2
H-6	-6,92	4	5	89	2	0	0	0
H-7	-7,22	1	3	97	0	0	0	0
H-8	-7,29	1	76	1	0	0	21	1
H-9	-7,3	0	22	0	0	1	72	4
H-10	-7,39	0	19	0	0	1	3	77

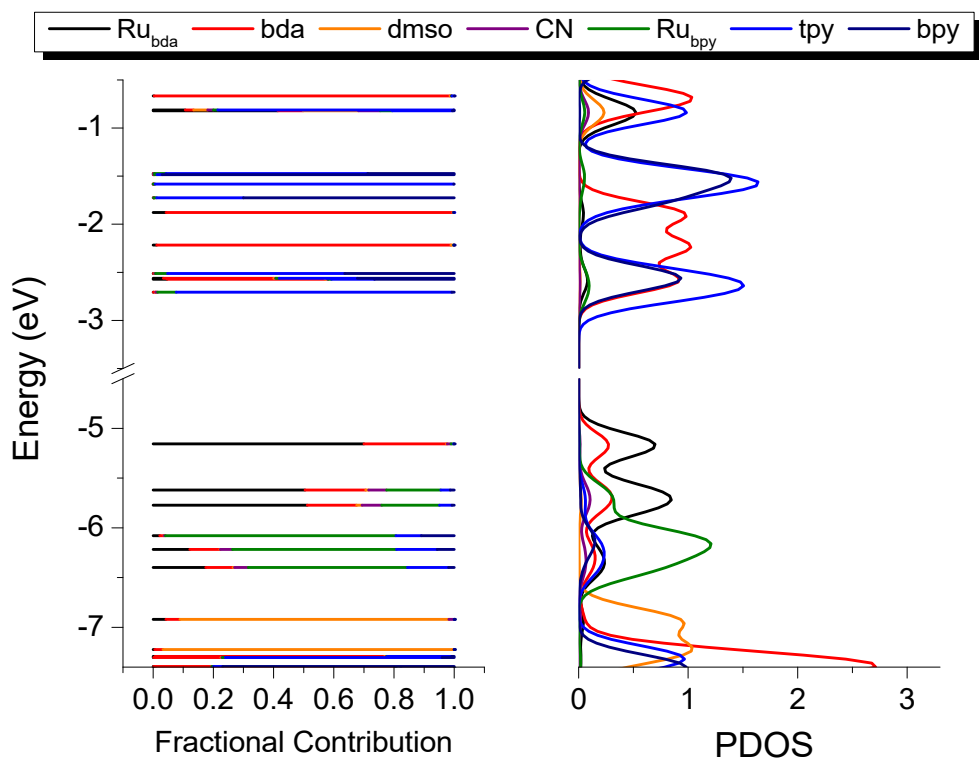


Figure S27. Molecular orbital diagram and partial density of states (PDOS) of complex $[\text{Ru}^{\text{II}}(\text{bpy})-\text{Ru}^{\text{II}}(\text{bda})]^+$ in their singlet ground state.

Table S2. (TD)DFT assignments for calculated UV-Vis transitions of the complex $[\text{Ru}^{\text{II}}(\text{bpy})-\text{Ru}^{\text{II}}(\text{bda})]^+$.

No.	Wavelength (nm)	Osc. Strength	Major contributions	Assignment
2	548.2	0.01	H-1 \rightarrow LUMO (71%) H-3 \rightarrow LUMO (12%)	$d(\text{Ru}_{\text{bda}}) \rightarrow \pi^*(\text{tpy})$
3	538.6	0.01	H-1 \rightarrow L+1 (83%)	$d(\text{Ru}_{\text{bda}}) \rightarrow \pi^*(\text{bda})$
11	479.0	0.01	H-2 \rightarrow L+1 (52%)	$d(\text{Ru}_{\text{bda}}) \rightarrow \pi^*(\text{bda})$
12	465.5	0.05	H-2 \rightarrow LUMO (35%) H-1 \rightarrow L+3 (17%)	$d(\text{Ru}_{\text{bda}}) \rightarrow \pi^*(\text{tpy})$ $d(\text{Ru}_{\text{bpy}}) \rightarrow \pi^*(\text{tpy})$

			H-3 -> L+3 (16%)	d(Ru _{bpy}) -> π*(bpy)
18	430.1	0.10	H-3 -> L+3 (36%) H-3 -> L+2 (20%)	d(Ru _{bpy}) -> π*(tpy) d(Ru _{bpy}) -> π*(bpy)
64	310.8	0.16	H-9 -> LUMO (62%) H-4 -> L+7 (17%)	π(tpy) -> π*(tpy)
76	297.3	0.14	H-4 -> L+7 (40%) H-11 -> LUMO (12%) H-9 ->LUMO (11%)	π(tpy) -> π*(tpy)
89	286.3	0.22	H-12 -> L+1 (47%) H-6 -> L+5 (11%)	π(bda) -> π*(bda)
104	278.3	0.19	H-12 -> L+2 (27%) H-11 ->L+3 (17%) H-12 -> L+3 (14%)	LLCT (bda->tpy+bpy)
164	241.1	0.10	H-9 ->L+7 (24%) HOMO -> L+17 (10%)	π(tpy) -> π*(tpy)
200	229.0	0.19	H-3 ->L+17 (21%) H-6 ->L+10 (13%)	d(Ru _{bpy}) -> π*(tpy)

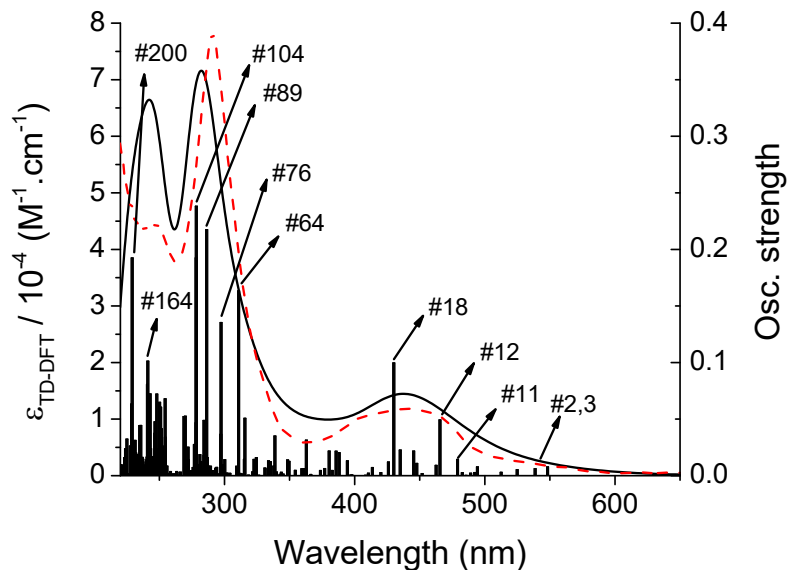


Figure S28. (TD)DFT-calculated (dashed curve) and experimental (solid curve) UV-visible absorption spectra of complex [Ru^{II}(bpy)-Ru^{II}(bda)]⁺ in their singlet ground state. Calculated transitions are represented by red vertical bars.

Table S3. Energies values and percentual group contributions of selected MO's of complex [Ru^{II}(MeO-bpy)CNRu^{II}(bda)]⁺ in their singlet ground state.

MO's	Energy (eV)	Ru _{bda}	bda	DMSO	CN	Ru _{tpy}	tpy	MeO-bpy
------	-------------	-------------------	-----	------	----	-------------------	-----	---------

L+10	-0,98	56	11	19	10	4	0	1
L+9	-1,28	0	0	0	0	1	0	98
L+8	-1,42	0	0	0	0	4	54	42
L+7	-1,56	0	0	0	0	1	99	0
L+6	-1,64	0	0	0	0	1	44	55
L+5	-1,94	3	96	0	0	0	0	0
L+4	-2,21	2	97	1	0	0	0	0
L+3	-2,36	0	0	0	0	3	4	92
L+2	-2,52	0	0	0	0	1	94	5
L+1	-2,59	7	89	1	0	0	2	0
LUMO	-2,68	0	2	0	1	6	90	1
HOMO	-5,54	69	24	0	2	4	1	0
H-1	-5,69	37	11	1	7	35	6	3
H-2	-5,85	45	13	2	6	27	6	1
H-3	-5,93	1	0	0	0	74	8	16
H-4	-6,21	30	16	1	4	35	9	5
H-5	-6,41	28	12	1	4	41	11	2
H-6	-6,93	5	5	89	2	0	0	0
H-7	-7,21	1	8	92	0	0	0	0
H-8	-7,24	1	91	6	0	0	2	0
H-9	-7,27	0	2	0	0	1	93	4
H-10	-7,32	1	98	0	0	0	1	0

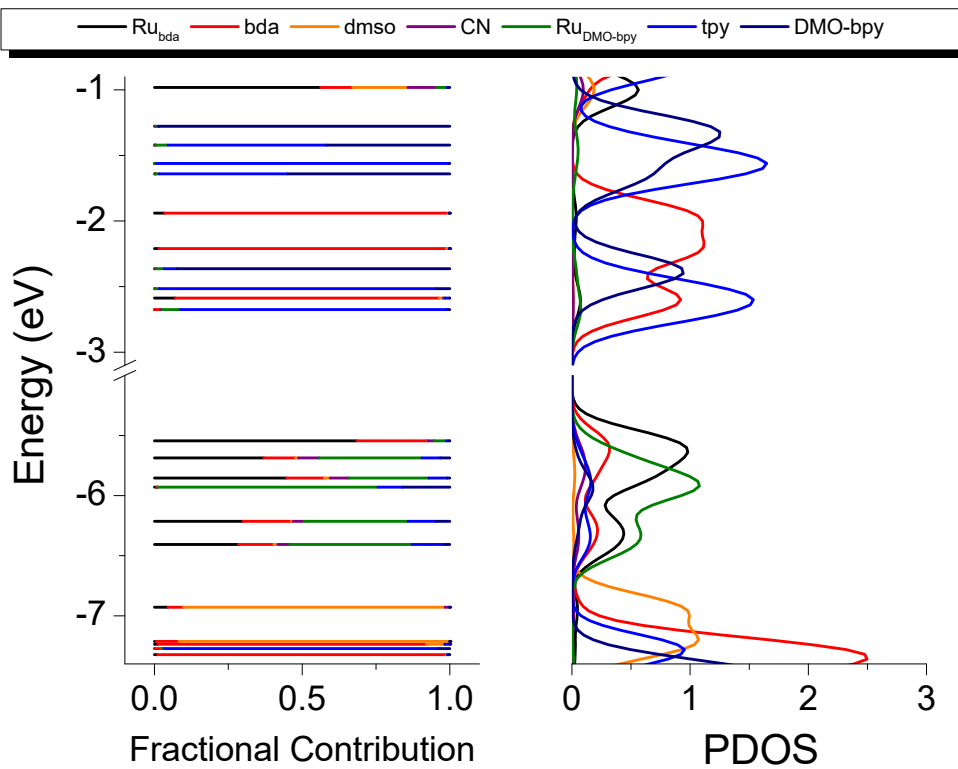


Figure S29. Molecular orbital diagram and partial density of states (PDOS) of complex $[\text{Ru}^{II}(\text{MeO-bpy})\text{CN}\text{Ru}^{II}(\text{bda})]^+$ in their singlet ground state.

Table S4. (TD)DFT assignments for calculated UV-Vis transitions of the complex **[Ru^{II}(MeO-bpy)CNRu^{II}(bda)]⁺**.

No.	Wavelength (nm)	Osc. Strength	Major contributions	Assignment
2	561.6	0.01	H-1 → LUMO (65%) H-3 → LUMO (19%)	d(Ru _{bda}) + d(Ru _{MeO-bpy}) → π*(tpy)
5	521.2	0.01	HOMO → LUMO (79%)	d(Ru _{bda}) → π*(tpy)
13	460.6	0.05	H-3 → L+2 (24%) H-2 → LUMO (21%) H-1 → L+2 (17%) H-1 → L+3 (12%)	d(Ru _{bda}) → π*(tpy) d(Ru _{MeO-bpy}) → π*(tpy)
17	429.4	0.09	H-3 → L+3 (55%) H-3 → L+1 (10%)	d(Ru _{MeO-bpy}) → π*(MeO-bpy)
63	310.6	0.10	H-9 → LUMO (65%) H-4 → L+7 (19%)	π(tpy) → π*(tpy)
88	286.5	0.12	H-11 → L+1 (44%) H-6 → L+5 (14%) H-11 → LUMO (14%)	LLCT π(bda) → π*(tpy)
91	284.4	0.12	H-13 → LUMO (69%)	LLCT π(MeO-bpy) → π*(tpy)
130	259.5	0.11	H-12 → L+1 (47%) H-6 → L+5 (11%)	LLCT π(MeO-bpy) → π*(tpy)
149	251.0	0.12	H-18 → LUMO (31%) H-14 → L+4 (27%)	π(tpy) → π*(tpy) π(bda) → π*(bda)

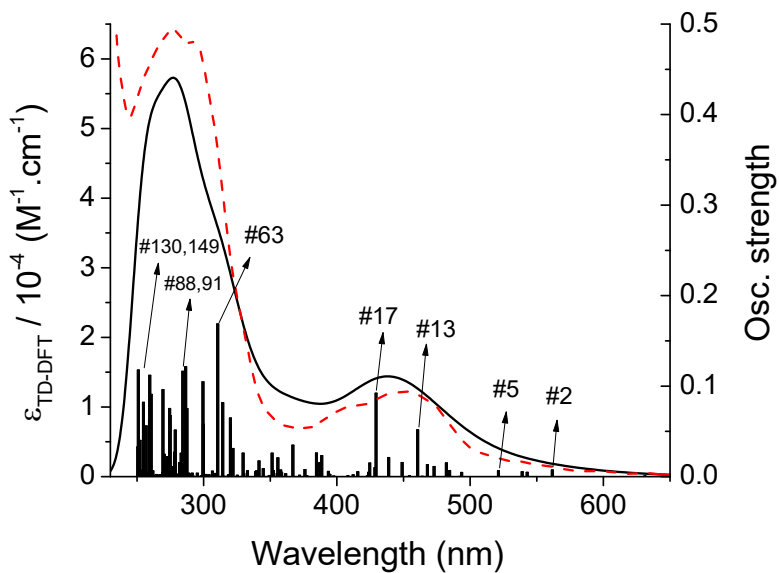


Figure S30. (TD)DFT-calculated (dashed curve) and experimental (solid curve) UV-visible absorption spectra of complex $[\text{Ru}^{\text{II}}(\text{MeO-bpy})\text{CNRu}^{\text{III}}(\text{bda})]^+$ in their triplet ground state. Calculated transitions are represented by red vertical bars.

Table S5. Energies values and percentual group contributions of selected α MO's of complex $[\text{Ru}^{\text{II}}(\text{bpy})\text{-Ru}^{\text{III}}(\text{bdaH})(\text{OH})]^{2+}$.

MO's (α)	Energy (eV)	Ru_{bda}	bdaH	DMSO	CN	Ru_{tpy}	tpy	bpy	OH
L+10	-1.57	1	0	0	0	3	59	36	0
L+9	-1.67	27	8	2	5	1	45	8	5
L+8	-1.68	23	6	2	4	1	56	4	4
L+7	-1.8	0	0	0	0	1	33	65	0
L+6	-2.12	59	31	9	1	0	0	0	0
L+5	-2.62	0	1	0	1	4	50	45	0
L+4	-2.64	1	40	0	0	1	25	33	0
L+3	-2.66	1	56	0	0	1	24	17	0
L+2	-2.78	1	97	0	0	0	2	0	0
L+1	-2.84	0	2	0	1	5	91	1	0
LUMO	-3.22	4	95	0	0	0	0	0	0
HOMO	-6.23	5	1	1	6	70	12	5	1
H-1	-6.33	2	0	0	2	72	11	12	0
H-2	-6.45	7	1	0	8	64	15	2	3
H-3	-7.02	43	18	4	2	6	2	0	24
H-4	-7.07	40	8	21	4	6	6	1	14
H-5	-7.4	1	0	2	0	1	82	13	0
H-6	-7.44	58	23	6	1	1	1	7	1
H-7	-7.47	5	2	0	0	2	12	79	0
H-8	-7.59	26	12	57	1	0	1	0	2
H-9	-7.66	2	1	96	0	0	0	0	0

H-10	-7.93	1	98	0	0	0	0	0	0
------	-------	---	----	---	---	---	---	---	---

Table S6. Energies values and percentual group contributions of selected β MO's of complex $[\text{Ru}^{\text{II}}(\text{bpy})\text{-Ru}^{\text{III}}(\text{bdaH})(\text{OH})]^{2+}$.

MO's (β)	Energy (eV)	Ru_{bda}	bdaH	DMSO	CN	Ru_{tpy}	tpy	bpy	OH
L+10	-1.58	7	3	0	2	2	27	59	1
L+9	-1.68	0	0	0	0	1	99	0	0
L+8	-1.8	0	0	0	0	1	33	65	0
L+7	-1.84	60	27	10	1	0	0	1	0
L+6	-2.56	7	86	1	0	0	4	1	1
L+5	-2.62	0	4	0	1	4	42	50	0
L+4	-2.65	0	1	0	0	1	54	44	0
L+3	-2.77	1	95	0	0	0	3	0	0
L+2	-2.83	0	4	0	1	5	89	1	0
L+1	-3.19	6	93	0	0	0	0	0	0
LUMO	-3.86	57	14	0	3	1	1	0	24
HOMO	-6.18	11	2	1	7	62	11	4	2
H-1	-6.31	2	0	0	1	74	10	12	0
H-2	-6.48	3	2	0	8	68	16	3	1
H-3	-6.87	43	10	11	4	14	7	1	12
H-4	-7.19	70	22	3	1	2	1	0	1
H-5	-7.4	0	0	1	0	1	85	13	0
H-6	-7.47	0	0	0	0	1	11	87	0
H-7	-7.51	15	7	72	0	0	1	0	5
H-8	-7.6	5	8	74	0	0	0	0	13
H-9	-7.84	6	40	24	0	0	0	0	28
H-10	-7.93	1	92	2	0	0	0	0	5

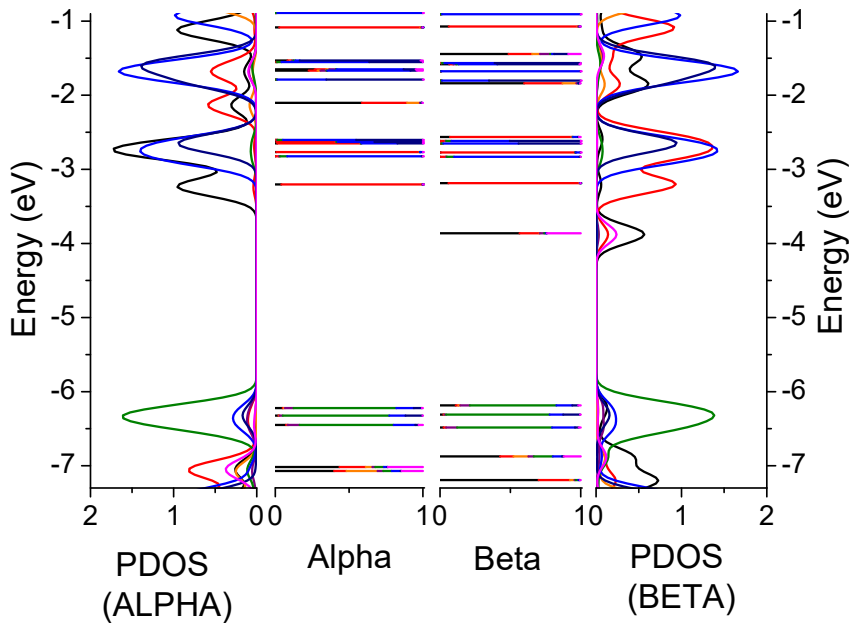


Figure S31. Molecular orbital diagram and partial density of states (PDOS) of complex $[\text{Ru}^{\text{II}}(\text{bpy})-\text{Ru}^{\text{III}}(\text{bdaH})(\text{OH})]^{2+}$.

Table S7. (TD)DFT assignments for calculated UV-Vis transitions of the complex $[\text{Ru}^{\text{II}}(\text{bpy})\text{CN}\text{Ru}^{\text{III}}(\text{bdaH})(\text{OH})]^{2+}$.

No.	Wavelength (nm)	Osc. Strength	Major contributions	Assignment
5	595.0	0.047	H-2(B) -> LUMO(B)	$d(\text{Ru}_{\text{tpy}}) \rightarrow d(\text{Ru}_{\text{bda}})$
22	458.8	0.026	H-9(B)->LUMO(B) (23%), H-8(B)->LUMO(B) (61%)	$\pi(\text{DMSO}) \rightarrow d(\text{Ru}_{\text{bda}})$
35	420.1	0.060	H-1(A)->L+3(A) (11%), H-1(A)->L+4(A) (15%), HOMO(A)->L+2(A) (12%), H-1(B)->L+4(B) (20%), HOMO(B)->L+6(B) (10%)	$d(\text{Ru}_{\text{tpy}}) \rightarrow \pi^*(\text{bda})$
134	306.7	0.063	H-5(A)->L+1(A) (12%), H-2(A)->L+8(A) (13%)	$d(\text{Ru}_{\text{tpy}}) \rightarrow \pi^*(\text{tpy})$
144	301.9	0.115	H-7(A)->L+1(A) (12%), H-6(B)->L+2(B) (19%), H-4(B)->L+4(B) (21%)	$d(\text{Ru}_{\text{tpy}}) \rightarrow \pi^*(\text{tpy})$
148	300.3	0.131	H-4(B)->L+4(B) (12%)	$d(\text{Ru}_{\text{bda}}) \rightarrow \pi^*(\text{tpy}) + \pi^*(\text{bpy})$

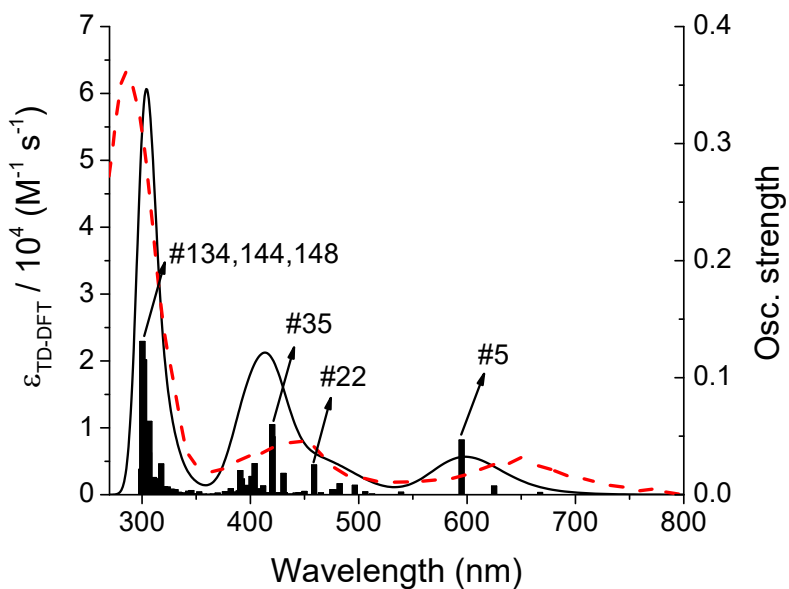


Figure S32. (TD)DFT-calculated (dashed curve) and experimental (solid curve) UV-visible absorption spectra of complex $[\text{Ru}^{\text{II}}(\text{bpy})\text{-}\text{Ru}^{\text{III}}(\text{bdaH})(\text{OH})]^{2+}$. Calculated transitions are represented by red vertical bars.

Table S8. Energies values and percentual group contributions of selected α MO's of complex $[\text{Ru}^{\text{II}}(\text{MeO-bpy})\text{-}\text{Ru}^{\text{III}}(\text{bdaH})(\text{OH})]^{2+}$.

MO's (α)	Energy (eV)	Ru_{bda}	bdaH	DMSO	CN	Ru_{tpy}	tpy	MeO-bpy	OH
L+10	-1.51	2	1	0	0	4	44	49	0
L+9	-1.65	8	3	1	1	1	84	1	2
L+8	-1.68	47	13	4	8	1	17	3	9
L+7	-1.72	0	0	0	0	1	52	46	0
L+6	-2.1	58	31	9	1	0	0	0	0
L+5	-2.44	0	0	0	1	2	2	95	0
L+4	-2.61	0	4	0	0	1	93	2	0
L+3	-2.66	2	92	1	0	0	4	1	0
L+2	-2.79	1	89	0	0	1	9	0	0
L+1	-2.81	0	10	0	1	5	83	1	0
LUMO	-3.22	4	95	0	0	0	0	0	0
HOMO	-6.11	2	0	0	3	73	10	12	0
H-1	-6.17	4	1	1	5	64	12	13	1
H-2	-6.4	6	1	0	8	65	15	2	2
H-3	-7.02	45	18	3	2	5	2	0	25
H-4	-7.06	41	9	21	4	4	4	2	14
H-5	-7.37	0	0	1	0	1	91	7	0
H-6	-7.46	63	26	6	1	1	1	1	1

H-7	-7.5	0	0	0	0	0	1	98	0
H-8	-7.59	20	9	51	1	0	0	16	2
H-9	-7.64	6	3	8	0	5	8	69	1
H-10	-7.67	2	1	96	0	0	0	0	0

Table S9. Energies values and percentual group contributions of selected β MO's of complex [Ru^{II}(MeO-bpy)-Ru^{III}(bdaH)(OH)]²⁺.

MO's (β)	Energy (eV)	Ru _{bda}	bdaH	DMSO	CN	Ru _{tpy}	tpy	MeO-bpy	OH
L+10	-1.53	12	4	1	3	2	35	41	2
L+9	-1.66	0	0	0	0	1	99	0	0
L+8	-1.72	0	0	0	0	1	52	47	0
L+7	-1.82	60	28	10	1	0	0	0	0
L+6	-2.44	0	0	0	1	2	2	95	0
L+5	-2.57	7	84	1	0	0	7	0	1
L+4	-2.62	0	6	0	0	1	90	2	0
L+3	-2.78	1	82	0	0	1	16	0	0
L+2	-2.81	0	18	0	1	4	76	1	0
L+1	-3.19	6	92	0	0	0	0	0	0
LUMO	-3.87	56	14	0	3	1	1	0	24
HOMO	-6.09	6	1	1	5	67	10	8	1
H-1	-6.14	4	1	0	3	66	10	16	1
H-2	-6.42	2	2	0	8	68	16	2	1
H-3	-6.85	46	10	11	4	9	5	3	13
H-4	-7.21	71	23	3	1	1	1	0	0
H-5	-7.37	0	0	0	0	1	92	7	0
H-6	-7.5	0	0	3	0	0	1	95	0
H-7	-7.53	14	6	70	0	0	0	5	4
H-8	-7.59	5	9	69	0	0	0	2	15
H-9	-7.63	1	1	3	0	4	8	83	0
H-10	-7.81	0	2	2	0	9	3	82	1

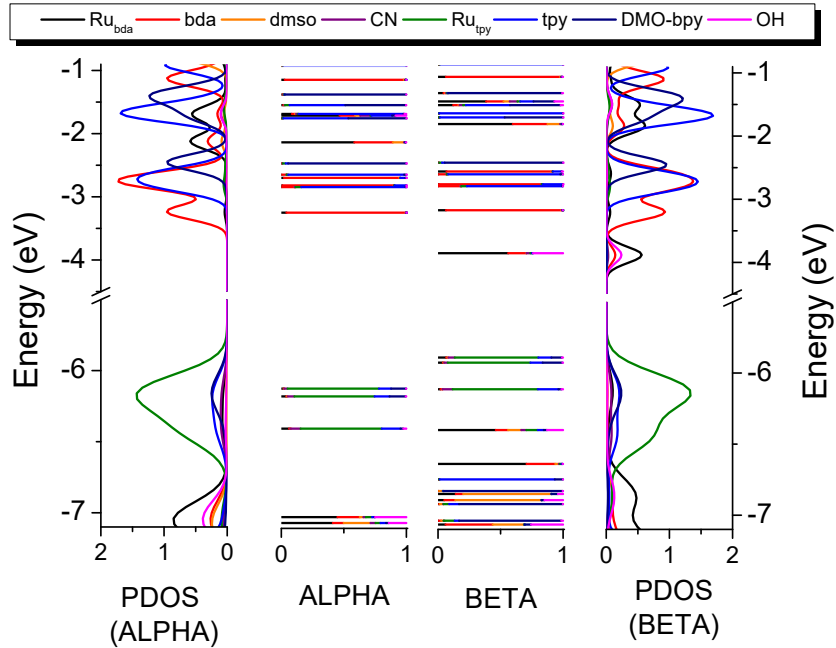


Figure S33. Molecular orbital diagram and partial density of states (PDOS) of complex $[\text{Ru}^{\text{II}}(\text{MeO-bpy})-\text{Ru}^{\text{III}}(\text{bdaH})(\text{OH})]^{2+}$.

Table S10. (TD)DFT assignments for calculated UV-Vis transitions of the complex $[\text{Ru}^{\text{II}}(\text{MeO-bpy})-\text{Ru}^{\text{III}}(\text{bdaH})(\text{OH})]^{2+}$.

No.	Wavelength (nm)	Osc. Strength	Major contributions	Assignment
5	616.5	0.054	H-2(B)->LUMO(B) (86%)	d(Ru _{tpy}) -> d(Ru _{bda})
22	460.7	0.025	H-8(B)->LUMO(B) (58%), H-11(B)->LUMO(B) (18%)	$\pi(\text{DMSO}) \rightarrow d(\text{Ru}_{\text{bda}})$
39	418.7	0.037	HOMO(A)->L+3(A) (27%)	d(Ru _{tpy}) -> $\pi^*(\text{bda})$
42	407.4	0.032	H-2(A)->L+4(A) (31%), H-2(B)->L+4(B) (39%)	d(Ru _{tpy}) -> $\pi^*(\text{tpy})$
139	305.7	0.158	H-5(A)->L+1(A) (15%), H-2(A)->L+9(A) (10%), H-5(B)->L+2(B) (13%), H-2(B)->L+9(B) (15%)	d(Ru _{tpy}) -> $\pi^*(\text{tpy})$

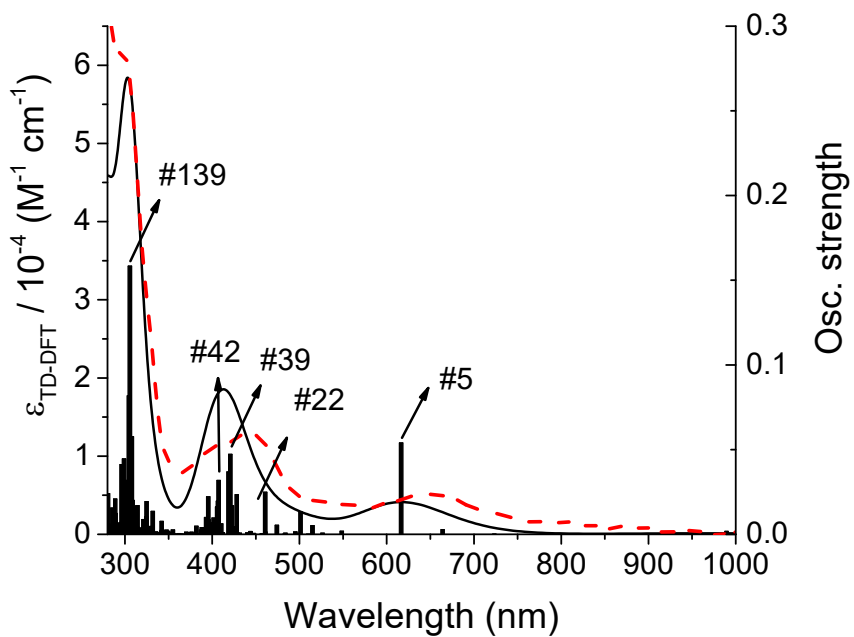


Figure S34. (TD)DFT-calculated (dashed curve) and experimental (solid curve) UV-visible absorption spectra of complex $[\text{Ru}^{\text{II}}(\text{MeO-bpy})\text{-Ru}^{\text{IV}}(\text{bdaH})(\text{OH})]^{2+}$. Calculated transitions are represented by red vertical bars.

Table S11. Energies values and percentual group contributions of selected MO's of complex $[\text{Ru}^{\text{II}}(\text{bpy})\text{-Ru}^{\text{IV}}(\text{bda})(\text{OH})]^{2+}$.

MO's	Energy (eV)	Ru_{bda}	bda	DMSO	CN	Ru_{tpy}	tpy	bpy	OH
L+10	-1.65	0	0	0	0	1	99	0	0
L+9	-1.78	0	0	0	0	1	30	69	0
L+8	-2.41	55	8	14	12	2	0	0	9
L+7	-2.58	0	0	0	0	4	58	37	0
L+6	-2.63	0	0	0	0	2	40	58	0
L+5	-2.71	1	97	0	0	0	1	0	0
L+4	-2.79	0	2	0	1	6	91	1	0
L+3	-2.87	1	97	0	0	0	1	0	0
L+2	-3.42	5	93	1	0	0	0	0	0
L+1	-3.56	55	31	1	1	0	0	0	13
LUMO	-3.89	60	32	0	0	0	0	0	8
HOMO	-6.17	1	0	0	4	77	11	7	0
H-1	-6.26	1	0	0	3	72	13	11	0
H-2	-6.37	2	0	0	8	71	16	2	0
H-3	-7.33	5	2	88	3	0	1	0	1
H-4	-7.37	1	0	1	0	1	91	6	0
H-5	-7.45	0	0	0	0	1	5	94	0
H-6	-7.6	6	6	87	0	0	0	0	1

H-7	-7.69	30	43	12	2	1	2	0	10
H-8	-7.78	7	64	1	1	0	0	0	28
H-9	-8.01	57	17	1	8	1	8	0	8
H-10	-8.04	1	99	0	0	0	0	0	0

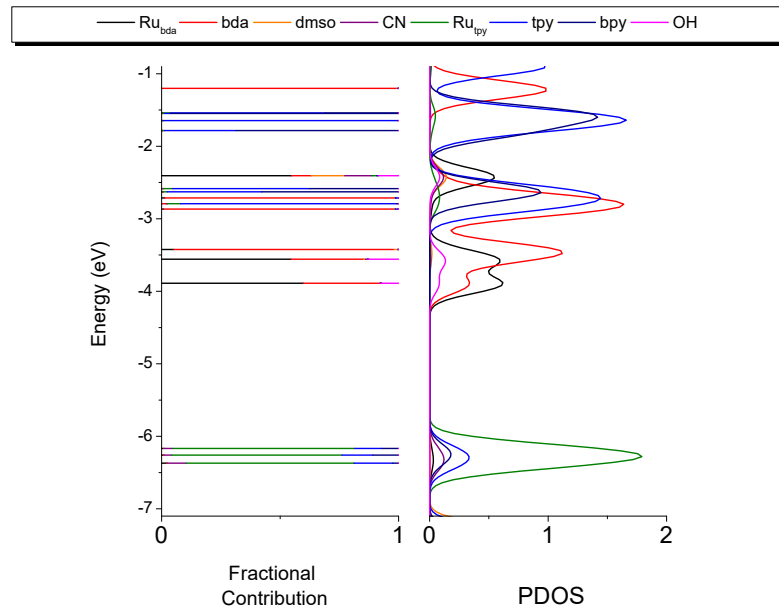


Figure S35. Molecular orbital diagram and partial density of states (PDOS) of complex $[\text{Ru}^{\text{II}}(\text{bpy})\text{-}\text{Ru}^{\text{IV}}(\text{bda})(\text{OH})]^{2+}$.

Table S12. (TD)DFT assignments for calculated UV-Vis transitions of the complex $[\text{Ru}^{\text{II}}(\text{bpy})\text{-}\text{Ru}^{\text{IV}}(\text{bda})(\text{OH})]^{2+}$.

No.	Wavelength (nm)	Osc. Strength	Major contributions	Assignment
13	488.3	0.011	H-1->L+4 (91%)	d(Ru _{tpy}) -> $\pi^*(\text{tpy})$
21	425.5	0.118	H-1->L+6 (79%)	d(Ru _{tpy}) -> $\pi^*(\text{tpy})$ d(Ru _{tpy}) -> $\pi^*(\text{bpy})$
33	396.3	0.034	H-1->L+7 (41%), H-2->L+4 (17%), H-8->LUMO (14%)	d(Ru _{tpy}) -> $\pi^*(\text{tpy})$ d(Ru _{tpy}) -> $\pi^*(\text{bpy})$
66	319.9	0.060	HOMO->L+11 (77%), H-1->L+12 (10%)	d(Ru _{tpy}) -> $\pi^*(\text{bpy})$
74	305.4	0.163	H-4->L+4 (31%), H-2->L+12 (21%), H-2->L+11 (16%)	d(Ru _{tpy}) -> $\pi^*(\text{tpy})$ d(Ru _{tpy}) -> $\pi^*(\text{bpy})$
81	300.6	0.175	H-1->L+12 (42%), H-3->L+8 (22%)	d(Ru _{tpy}) -> $\pi^*(\text{tpy})$

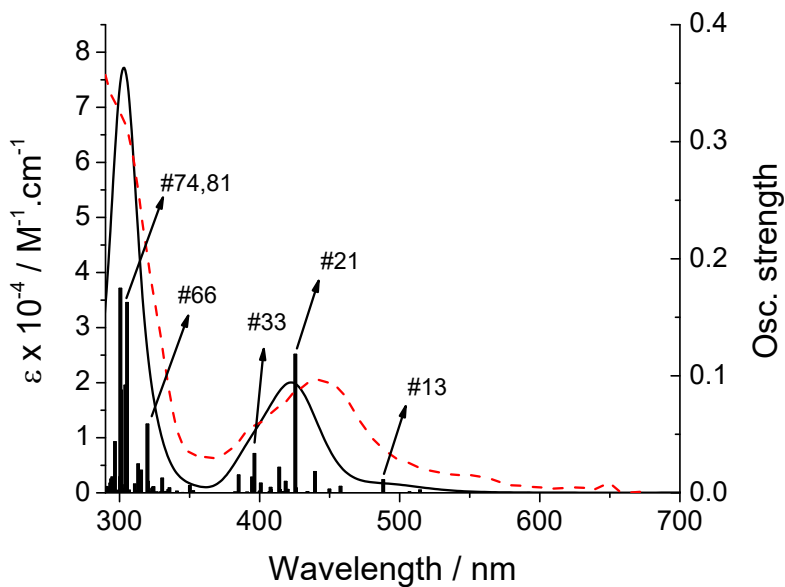


Figure S36. (TD)DFT-calculated (dashed curve) and experimental (solid curve) UV-visible absorption spectra of complex $[\text{Ru}^{\text{II}}(\text{bpy})\text{-}\text{Ru}^{\text{IV}}(\text{bda})(\text{OH})]^{2+}$. Calculated transitions are represented by red vertical bars.

Table S13. Energies values and percentual group contributions of selected MO's of complex $[\text{Ru}^{\text{II}}(\text{MeO-bpy})\text{-}\text{Ru}^{\text{IV}}(\text{bda})(\text{OH})]^{2+}$.

MO's	Energy (eV)	Ru_{bda}	bda	DMSO	CN	Ru_{tpy}	tpy	MeO-bpy	OH
L+10	-1.62	0	0	0	0	1	99	0	0
L+9	-1.7	0	0	0	0	1	46	52	0
L+8	-2.39	52	8	13	11	2	0	6	8
L+7	-2.42	3	0	1	1	2	3	89	0
L+6	-2.58	0	1	0	0	1	95	3	0
L+5	-2.71	1	96	0	0	0	3	0	0
L+4	-2.76	0	3	0	1	6	90	1	0
L+3	-2.86	1	98	0	0	0	1	0	0
L+2	-3.42	5	93	1	0	0	0	0	0
L+1	-3.55	55	30	1	1	0	0	0	13
LUMO	-3.88	60	32	0	0	0	0	0	8
HOMO	-6.03	0	0	0	1	76	9	14	0
H-1	-6.11	1	0	0	6	67	14	11	0
H-2	-6.29	2	0	0	8	71	17	2	0
H-3	-7.32	5	2	83	3	0	6	0	1
H-4	-7.34	1	0	6	0	1	88	4	0
H-5	-7.49	0	0	0	0	0	0	99	0
H-6	-7.59	8	8	51	1	0	1	29	1
H-7	-7.61	0	0	37	0	2	4	56	0
H-8	-7.69	28	41	11	2	1	2	5	9

H-9	-7.77	7	63	1	1	0	0	0	28
H-10	-7.8	0	0	0	0	9	3	88	0

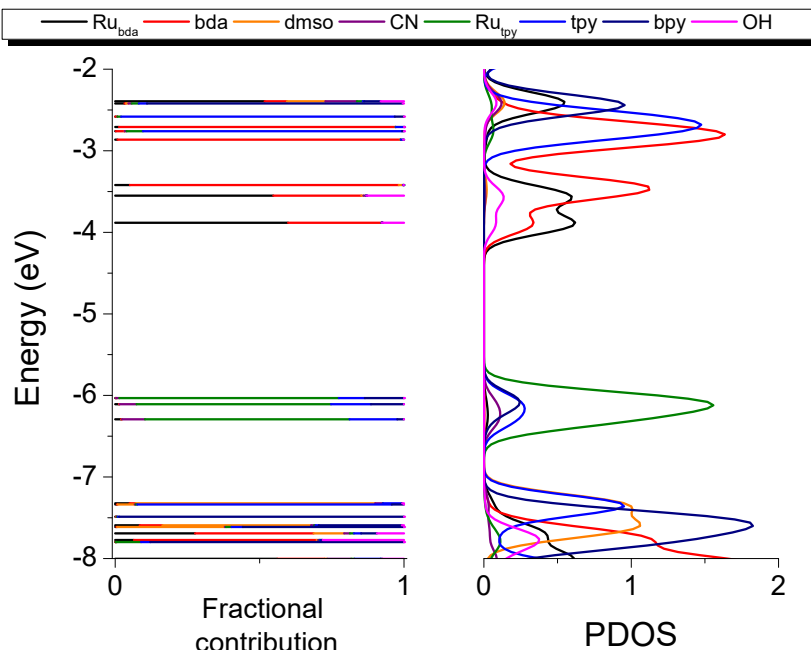


Figure S37. Molecular orbital diagram and partial density of states (PDOS) of complex $[\text{Ru}^{\text{II}}(\text{MeO-bpy})-\text{Ru}^{\text{IV}}(\text{bda})(\text{OH})]^{2+}$.

Table S14. (TD)DFT assignments for calculated UV-Vis transitions of the complex $[\text{Ru}^{\text{II}}(\text{MeO-bpy})-\text{Ru}^{\text{IV}}(\text{bda})(\text{OH})]^{2+}$.

No.	Wavelength (nm)	Osc. Strength	Major contributions	Assignment
13	507.9	0.014	H-1->L+4 (95%)	$d(\text{Ru}_{\text{tpy}}) \rightarrow \pi^*(\text{tpy})$
20	437.5	0.027	HOMO->L+7 (80%)	$d(\text{Ru}_{\text{tpy}}) \rightarrow \pi^*(\text{MeO-bpy})$
22	426.3	0.103	H-1->L+6 (39%), H-1->L+7 (32%), H-2->L+4 (20%)	$d(\text{Ru}_{\text{tpy}}) \rightarrow \pi^*(\text{tpy})$ $d(\text{Ru}_{\text{tpy}}) \rightarrow \pi^*(\text{MeO-bpy})$
33	401.9	0.037	H-1->L+7 (36%), H-2->L+7 (16%), H-2->L+4 (15%)	$d(\text{Ru}_{\text{tpy}}) \rightarrow \pi^*(\text{MeO-bpy})$ $d(\text{Ru}_{\text{tpy}}) \rightarrow \pi^*(\text{tpy})$
38	385.0	0.016	H-3->L+2 (88%)	$\pi(\text{DMSO}) \rightarrow \pi^*(\text{bda})$
79	307.1	0.175	H-4->L+4 (27%), H-4->L+3 (24%), H-1->L+17 (16%)	$\pi(\text{tpy}) \rightarrow \pi^*(\text{tpy})$ $\pi(\text{tpy}) \rightarrow \pi^*(\text{bda})$
81	306.3	0.212	H-4->L+4 (41%), H-4->L+3 (18%), H-1->L+10 (11%)	$\pi(\text{tpy}) \rightarrow \pi^*(\text{tpy})$ $\pi(\text{tpy}) \rightarrow \pi^*(\text{bda})$
83	302.6	0.218	H-1->L+11 (36%), H-1->L+12 (19%),	$d(\text{Ru}_{\text{tpy}}) \rightarrow \pi^*(\text{MeO-bpy})$

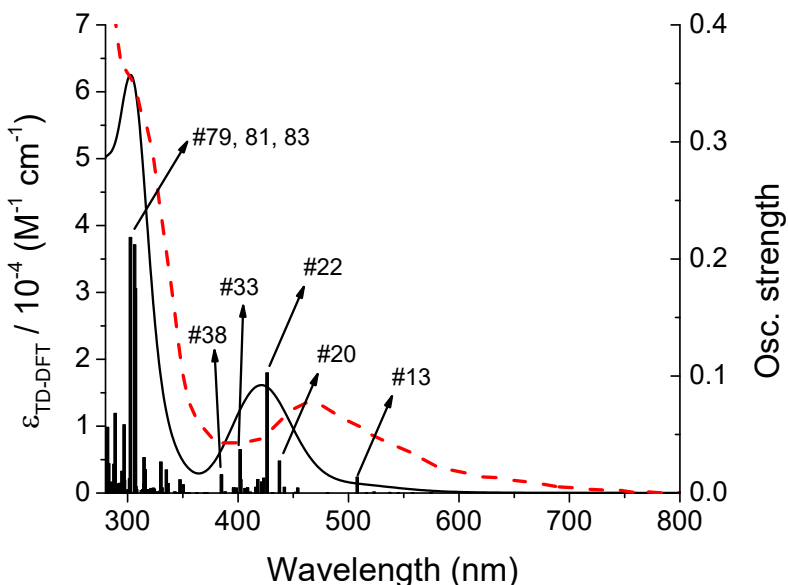


Figure S38. (TD)DFT-calculated (dashed curve) and experimental (solid curve) UV-visible absorption spectra of complex $[\text{Ru}^{\text{II}}(\text{MeO-bpy})\text{-Ru}^{\text{IV}}(\text{bda})(\text{OH})]^{2+}$. Calculated transitions are represented by red vertical bars.

Table S15. Energies values and percentual group contributions of selected α MO's of complex $[\text{Ru}^{\text{III}}(\text{bpy})\text{-Ru}^{\text{IV}}(\text{bda})(\text{OH})]^{3+}$.

MO's (α)	Energy (eV)	Ru _{bda}	bda	DMSO	CN	Ru _{tpy}	tpy	bpy	OH
L+10	-2.29	0	0	0	0	1	55	44	0
L+9	-2.44	5	1	1	2	45	41	5	1
L+8	-2.71	48	10	13	10	7	3	2	8
L+7	-2.79	2	98	0	0	0	0	0	0
L+6	-2.93	2	96	1	0	0	1	0	1
L+5	-3.12	0	1	0	0	1	91	8	0
L+4	-3.2	0	0	0	0	2	8	90	0
L+3	-3.46	0	4	0	0	3	91	1	0
L+2	-3.51	6	88	2	0	0	5	0	0
L+1	-3.71	54	32	1	1	0	0	0	13
LUMO	-4.03	59	33	0	0	0	0	0	8
HOMO	-7.44	6	2	88	2	0	0	0	1
H-1	-7.7	6	6	84	1	1	1	0	1
H-2	-7.77	9	9	8	2	8	57	4	2
H-3	-7.81	18	33	6	1	2	27	0	13
H-4	-7.88	6	46	1	1	1	6	22	18
H-5	-7.89	4	17	0	0	1	1	72	5
H-6	-8.05	37	10	1	9	23	12	4	4

H-7	-8.11	1	98	0	0	0	1	0	0
H-8	-8.24	2	9	0	3	48	24	14	0
H-9	-8.26	2	96	0	0	1	0	0	0
H-10	-8.36	14	11	0	2	33	29	9	2

Table S16. Energies values and percentual group contributions of selected β MO's of complex [Ru^{III}(bpy)-Ru^{IV}(bda)(OH)]³⁺.

MO's (β)	Energy (eV)	Ru _{bda}	bda	DMSO	CN	Ru _{tpy}	tpy	bpy	OH
L+10	-2.25	1	0	0	1	25	69	3	0
L+9	-2.67	53	10	14	10	4	1	1	9
L+8	-2.79	1	98	0	0	0	0	0	0
L+7	-2.93	1	95	0	0	0	2	0	0
L+6	-3.06	0	2	0	0	3	77	18	0
L+5	-3.17	0	0	0	0	3	19	78	0
L+4	-3.44	0	2	0	0	3	94	1	0
L+3	-3.5	6	90	2	0	0	2	0	0
L+2	-3.71	54	32	1	1	0	0	0	13
L+1	-4.03	59	33	0	0	0	0	0	8
LUMO	-5.28	0	0	0	3	74	15	7	0
HOMO	-7.44	6	2	88	2	0	0	0	1
H-1	-7.68	11	10	51	2	12	10	3	1
H-2	-7.72	2	1	37	1	20	34	4	0
H-3	-7.78	21	28	11	3	11	17	0	9
H-4	-7.87	4	59	0	1	2	6	1	27
H-5	-7.89	2	1	0	1	5	7	82	1
H-6	-7.91	12	4	0	5	26	31	20	2
H-7	-8.02	6	21	0	2	37	26	6	0
H-8	-8.11	2	97	0	0	0	0	0	0
H-9	-8.26	3	95	0	0	0	0	0	1
H-10	-8.29	41	24	1	3	12	12	2	6

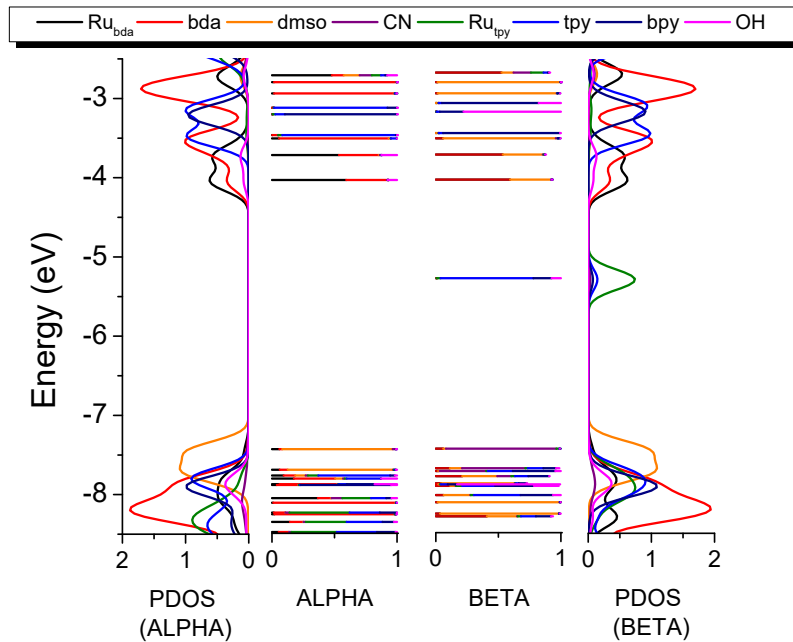


Figure S39. Molecular orbital diagram and partial density of states (PDOS) of complex $[\text{Ru}^{\text{III}}(\text{bpy})\text{-}\text{Ru}^{\text{IV}}(\text{bda})(\text{OH})]^{3+}$.

Table S17. (TD)DFT assignments for calculated UV-Vis transitions of the complex $[\text{Ru}^{\text{III}}(\text{bpy})\text{-}\text{Ru}^{\text{IV}}(\text{bda})(\text{OH})]^{3+}$.

No.	Wavelength (nm)	Osc. Strength	Major contributions	Assignment
7	669.1	0.005	H-5(B)->LUMO(B) (73%), H-6(B)->LUMO(B) (24%)	$\pi(\text{bpy}) \rightarrow d(\text{Ru}_{\text{tpy}})$
9	619.9	0.005	H-1(B)->LUMO(B) (44%), H-3(B)->LUMO(B) (29%), H-7(B)->LUMO(B) (23%)	$\pi(\text{DMSO}) \rightarrow d(\text{Ru}_{\text{tpy}})$ $\pi(\text{bda}) \rightarrow d(\text{Ru}_{\text{tpy}})$
15	525.3	0.011	H-10(B)->LUMO(B) (82%)	$d(\text{Ru}_{\text{bda}}) \rightarrow d(\text{Ru}_{\text{tpy}})$
41	396.0	0.013	H-17(B)->LUMO(B) (72%)	$\pi(\text{tpy}) \rightarrow d(\text{Ru}_{\text{tpy}})$
46	382.4	0.017	HOMO(B)->L+3(B) (48%), HOMO(A)->L+2(A) (47%)	$\pi(\text{DMSO}) \rightarrow \pi^*(\text{bda})$
49	377.9	0.016	H-19(B)->LUMO(B) (57%)	$\pi(\text{bpy}) \rightarrow d(\text{Ru}_{\text{tpy}})$
103	327.0	0.033	H-5(A)->L+1(A) (24%)	$\pi(\text{bpy}) \rightarrow d(\text{Ru}_{\text{bda}})$
134	313.0	0.040	H-2(B)->L+4(B) (15%), H-1(B)->L+4(B) (13%)	$\pi(\text{DMSO}) \rightarrow \pi^*(\text{tpy})$
149	307.0	0.023	H-24(B)->LUMO(B) (18%), H-23(B)->LUMO(B) (23%)	$\pi(\text{DMSO}) \rightarrow d(\text{Ru}_{\text{tpy}})$ $\pi(\text{bda}) \rightarrow d(\text{Ru}_{\text{tpy}})$

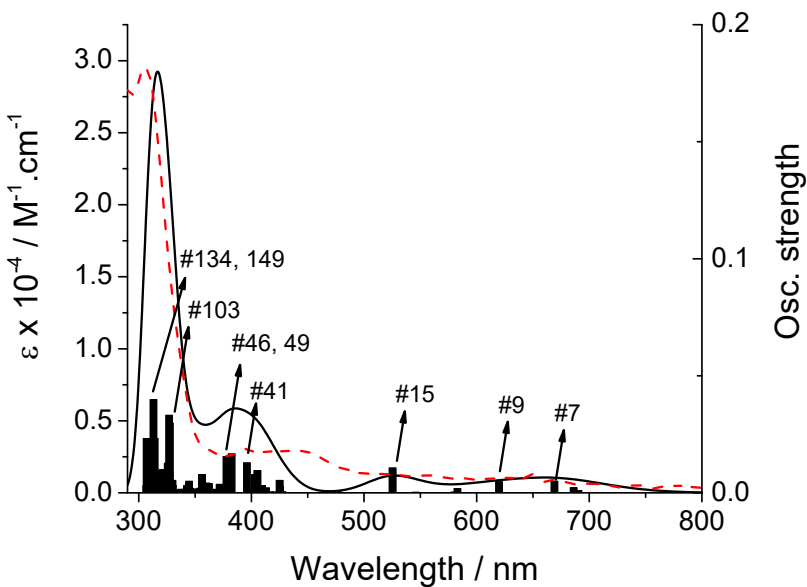


Figure S40. (TD)DFT-calculated (dashed curve) and experimental (solid curve) UV-visible absorption spectra of complex $[\text{Ru}^{\text{III}}(\text{bpy})\text{-Ru}^{\text{IV}}(\text{bda})(\text{OH})]^{3+}$. Calculated transitions are represented by red vertical bars.

Table S18. Energies values and percentual group contributions of selected α MO's of complex $[\text{Ru}^{\text{III}}(\text{MeO-bpy})\text{-Ru}^{\text{IV}}(\text{bda})(\text{OH})]^{3+}$.

MO's (α)	Energy (eV)	Ru_{bda}	bda	DMSO	CN	Ru_{tpy}	tpy	MeO-bpy	OH
L+10	-2.23	0	0	0	0	1	63	36	0
L+9	-2.36	3	0	1	2	47	41	5	0
L+8	-2.67	50	9	13	10	6	2	1	8
L+7	-2.79	1	98	0	0	0	0	0	0
L+6	-2.93	1	92	0	0	0	2	4	0
L+5	-2.94	0	4	0	0	1	1	93	0
L+4	-3.08	0	2	0	0	1	96	1	0
L+3	-3.41	0	1	0	0	3	94	1	0
L+2	-3.5	6	91	2	0	0	1	0	0
L+1	-3.7	54	32	1	1	0	0	0	13
LUMO	-4.02	59	33	0	0	0	0	0	8
HOMO	-7.42	6	2	88	2	0	0	0	1
H-1	-7.56	5	2	1	3	24	14	51	0
H-2	-7.69	4	5	87	0	1	1	2	1
H-3	-7.77	1	1	1	0	11	40	45	0
H-4	-7.79	22	33	10	2	3	19	2	10
H-5	-7.81	3	6	1	0	3	28	55	3
H-6	-7.87	8	63	1	1	1	0	2	24
H-7	-7.95	3	1	0	1	3	3	88	0
H-8	-8.03	30	11	1	8	24	11	13	3

H-9	-8.11	1	97	0	0	0	0	0	0
H-10	-8.25	6	75	0	1	8	7	2	1

Table S19. Energies values and percentual group contributions of selected β MO's of complex [Ru^{III}(MeO-bpy)-Ru^{IV}(bda)(OH)]³⁺.

MO's (β)	Energy (eV)	Ru _{bda}	bda	DMSO	CN	Ru _{tpy}	tpy	MeO-bpy	OH
L+10	-2.18	0	0	0	1	21	75	3	0
L+9	-2.64	53	9	14	10	3	1	1	9
L+8	-2.79	1	98	0	0	0	0	0	0
L+7	-2.88	0	1	0	0	3	5	91	0
L+6	-2.93	1	94	0	0	0	2	1	0
L+5	-3.05	0	2	0	0	2	92	3	0
L+4	-3.39	0	1	0	0	3	95	1	0
L+3	-3.5	6	91	2	0	0	1	0	0
L+2	-3.69	54	32	1	1	0	0	0	13
L+1	-4.01	59	33	0	0	0	0	0	8
LUMO	-5.15	0	0	0	2	73	13	11	0
HOMO	-7.39	4	1	10	4	35	11	36	0
H-1	-7.43	5	2	79	2	4	2	5	1
H-2	-7.68	8	8	76	1	4	2	1	1
H-3	-7.75	19	18	23	5	22	8	1	5
H-4	-7.79	0	0	0	0	1	73	25	0
H-5	-7.85	3	42	0	2	14	6	8	25
H-6	-7.87	5	20	0	1	3	11	52	7
H-7	-7.92	14	28	1	2	14	8	32	1
H-8	-8.02	1	4	0	1	6	8	80	0
H-9	-8.11	1	98	0	0	0	0	0	0
H-10	-8.24	41	24	1	3	8	7	10	7

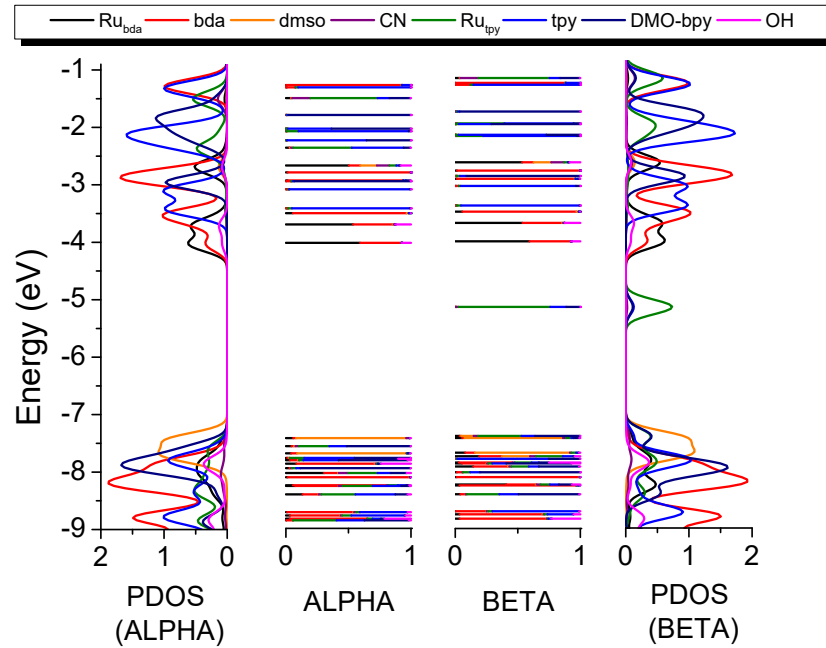


Figure S41. Molecular orbital diagram and partial density of states (PDOS) of complex $[\text{Ru}^{\text{III}}(\text{MeO-bpy})-\text{Ru}^{\text{IV}}(\text{bda})(\text{OH})]^{3+}$.

Table S20. (TD)DFT assignments for calculated UV-Vis transitions of the complex $[\text{Ru}^{\text{III}}(\text{MeO-bpy})-\text{Ru}^{\text{IV}}(\text{bda})(\text{OH})]^{3+}$.

No.	Wavelength (nm)	Osc. Strength	Major contributions	Assignment
9	594.2	0.023	H-8(B)->LUMO(B) (44%), H-6(B)->LUMO(B) (12%), H-7(B)->LUMO(B) (11%), H-2(B)->LUMO(B) (10%)	$\pi(\text{MeO-bpy}) \rightarrow d(\text{Ru}_{\text{tpy}})$
16	528.0	0.070	H-12(B)->LUMO(B) (62%), H-10(B)->LUMO(B) (14%)	$\pi(\text{MeO-bpy}) \rightarrow d(\text{Ru}_{\text{tpy}})$
29	424.1	0.008	HOMO(A)->L+1(A) (46%), H-1(B)->L+2(B) (41%)	$\pi(\text{DMSO}) \rightarrow d(\text{Ru}_{\text{bda}})$
38	403.2	0.008	H-6(A)->LUMO(A) (32%), H-5(B)->L+1(B) (24%)	$\pi(\text{bda}) \rightarrow d(\text{Ru}_{\text{bda}})$ $\pi(\text{OH}) \rightarrow d(\text{Ru}_{\text{bda}})$
46	382.9	0.016	HOMO(A)->L+2(A) (48%), H-1(B)->L+3(B) (40%)	$\pi(\text{DMSO}) \rightarrow \pi^*(\text{bda})$
118	321.5	0.037	H-5(A)->L+3(A) (17%)	$\pi(\text{tpy}) \rightarrow \pi^*(\text{tpy})$ $\pi(\text{MeO-bpy}) \rightarrow \pi^*(\text{tpy})$
165	303.5	0.062	HOMO(A)->L+8(A) (19%), H-1(B)->L+9(B) (15%)	$\pi(\text{DMSO}) \rightarrow d(\text{Ru}_{\text{bda}})$
181	296.6	0.052	H-8(A)->L+4(A) (15%), H-4(A)->L+4(A) (15%)	$d(\text{Ru}_{\text{bda}}) \rightarrow \pi(\text{tpy})$

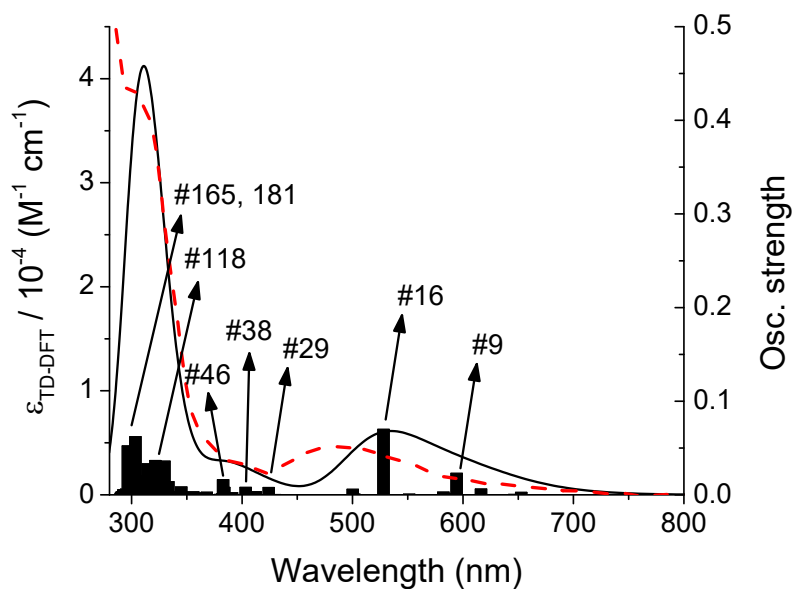


Figure S42. (TD)DFT-calculated (dashed curve) and experimental (solid curve) UV-visible absorption spectra of complex $[\text{Ru}^{\text{III}}(\text{MeO-bpy})-\text{Ru}^{\text{IV}}(\text{bda})(\text{OH})]^{3+}$. Calculated transitions are represented by red vertical bars.

Table S21. Energies values and percentual group contributions of selected α MO's of complex $[\text{Ru}^{\text{III}}(\text{bpy})-\text{Ru}^{\text{V}}(\text{bda})(\text{O})]^{3+}$.

MO's (α)	Energy (eV)	Ru _{bda}	bda	DMSO	CN	Ru _{tpy}	tpy	bpy	O
L+10	-2.3	0	0	0	0	1	55	44	0
L+9	-2.49	1	0	0	2	50	41	6	0
L+8	-2.8	1	99	0	0	0	0	0	0
L+7	-2.89	27	50	5	5	2	1	1	9
L+6	-2.95	23	58	4	3	1	1	0	9
L+5	-3.13	0	1	0	0	1	90	8	0
L+4	-3.21	0	0	0	0	2	8	90	0
L+3	-3.47	0	12	0	0	3	84	1	0
L+2	-3.52	3	84	1	0	0	12	0	1
L+1	-3.96	55	28	7	5	1	0	0	4
LUMO	-4.51	56	32	0	0	0	0	0	12
HOMO	-7.66	6	3	86	3	0	0	0	2
H-1	-7.79	1	0	0	1	7	88	3	0
H-2	-7.9	0	0	1	0	1	4	94	0
H-3	-7.92	1	7	90	0	0	0	1	0
H-4	-8.03	1	86	1	0	0	0	0	11
H-5	-8.06	19	59	6	2	6	3	2	2
H-6	-8.13	7	85	1	1	3	2	1	0
H-7	-8.18	16	18	1	6	31	16	5	6
H-8	-8.25	2	78	0	1	11	5	4	0
H-9	-8.29	4	21	0	3	39	24	9	1

H-10	-8.44	16	7	1	2	28	25	13	7
------	-------	----	---	---	---	----	----	----	---

Table S22. Energies values and percentual group contributions of selected β MO's of complex $[\text{Ru}^{\text{III}}(\text{bpy})\text{-Ru}^{\text{V}}(\text{bda})(\text{O})]^{3+}$.

MO's (β)	Energy (eV)	Ru_{bda}	bda	DMSO	CN	Ru_{tpy}	tpy	bpy	O
L+10	-2.71	49	10	10	7	2	1	1	22
L+9	-2.8	1	99	0	0	0	0	0	0
L+8	-2.92	1	96	0	0	0	2	0	1
L+7	-3.07	0	2	0	0	3	76	19	0
L+6	-3.18	0	0	0	0	3	20	77	0
L+5	-3.4	5	84	0	0	0	4	0	6
L+4	-3.45	0	3	0	0	3	92	1	0
L+3	-3.78	56	25	6	6	1	0	0	6
L+2	-4.3	54	26	0	0	0	0	0	20
L+1	-4.81	28	11	4	1	1	0	0	55
LUMO	-5.32	0	0	0	3	74	14	8	1
HOMO	-7.65	7	3	83	3	3	1	0	1
H-1	-7.75	1	1	2	1	25	63	6	0
H-2	-7.85	2	71	1	0	1	2	0	23
H-3	-7.9	1	3	3	0	2	4	87	0
H-4	-7.91	5	14	60	1	4	5	11	0
H-5	-7.95	7	10	30	3	21	22	6	0
H-6	-8.01	2	3	2	5	51	31	6	1
H-7	-8.1	2	78	4	0	8	6	1	0
H-8	-8.15	14	64	0	1	12	7	1	0
H-9	-8.27	1	98	0	0	0	0	0	1
H-10	-8.67	4	91	1	1	0	1	0	2

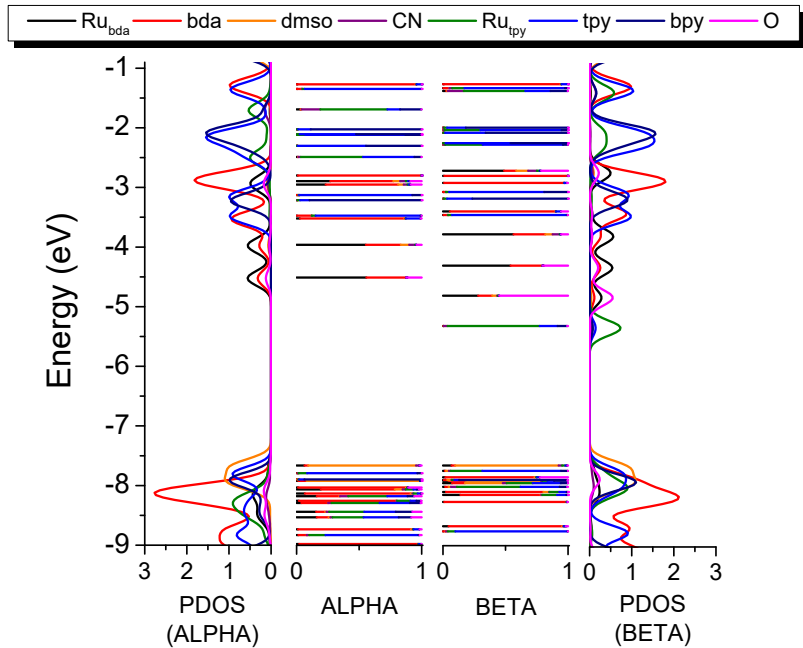


Figure S43. Molecular orbital diagram and partial density of states (PDOS) of complex $[\text{Ru}^{\text{III}}(\text{bpy})\text{-Ru}^{\text{V}}(\text{bda})(\text{O})]^{3+}$.

Table S23. (TD)DFT assignments for calculated UV-Vis transitions of the complex $[\text{Ru}^{\text{III}}(\text{bpy})\text{CN}\text{Ru}^{\text{V}}(\text{bda})(\text{O})]^{3+}$.

No.	Wavelength (nm)	Osc. Strength	Major contributions	Assignment
7	680.3	0.005	H-3(B)->LUMO(B) (78%), H-4(B)->LUMO(B) (13%)	$\pi(\text{bpy}) \rightarrow d(\text{Ru}_{\text{tpy}})$
9	634.8	0.008	HOMO(B)->LUMO(B) (67%), HOMO(B)->L+1(B) (26%)	$\pi(\text{DMSO}) \rightarrow d(\text{Ru}_{\text{tpy}})$
15	560.0	0.004	H-4(B)->LUMO(B) (53%), H-8(B)->LUMO(B) (17%), H-7(B)->LUMO(B) (17%)	$\pi(\text{DMSO}) \rightarrow d(\text{Ru}_{\text{tpy}})$
24	490.2	0.004	H-7(A)->L+1(A) (24%), H-10(A)->L+1(A) (16%), H-11(A)->L+1(A) (14%), HOMO(A)->L+1(A) (10%)	$d(\text{Ru}_{\text{tpy}}) \rightarrow d(\text{Ru}_{\text{bda}})$
51	403.2	0.024	HOMO(B)->L+3(B) (27%), HOMO(A)->L+1(A) (20%)	$\pi(\text{DMSO}) \rightarrow d(\text{Ru}_{\text{bda}})$
54	397.8	0.024	H-3(A)->L+1(A) (19%), HOMO(B)->L+3(B) (15%), H-20(B)->L+1(B) (11%)	$\pi(\text{DMSO}) \rightarrow d(\text{Ru}_{\text{bda}})$
66	380.8	0.014	H-18(B)->LUMO(B) (68%)	$\pi(\text{bpy}) \rightarrow d(\text{Ru}_{\text{tpy}})$

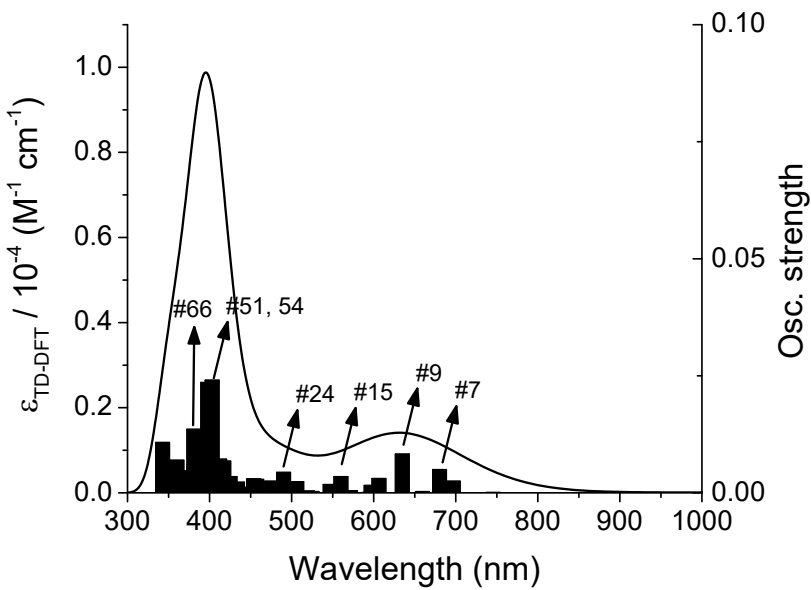


Figure S44. (TD)DFT-calculated UV-visible absorption spectra of complex $[\text{Ru}^{\text{III}}(\text{bpy})-\text{Ru}^{\text{V}}(\text{bda})(\text{O})]^{3+}$. Calculated transitions are represented by black vertical bars.

Table S24. Energies values and percentual group contributions of selected α MO's of complex $[\text{Ru}^{\text{III}}(\text{MeO-bpy})-\text{Ru}^{\text{V}}(\text{bda})(\text{O})]^{3+}$.

MO's (α)	Energy (eV)	Ru_{bda}	bda	DMSO	CN	Ru_{tpy}	tpy	MeO-bpy	O
L+10	-2.23	0	0	0	0	1	62	37	0
L+9	-2.4	1	0	0	2	51	40	6	0
L+8	-2.79	1	99	0	0	0	0	0	0
L+7	-2.87	37	34	7	6	2	1	1	13
L+6	-2.94	13	70	2	1	0	1	7	5
L+5	-2.95	1	5	0	0	1	1	90	1
L+4	-3.09	0	1	0	0	1	97	1	0
L+3	-3.42	0	3	0	0	3	93	1	0
L+2	-3.5	3	92	1	0	0	3	0	1
L+1	-3.94	55	28	7	5	1	0	0	4
LUMO	-4.5	56	32	0	0	0	0	0	12
HOMO	-7.59	1	0	0	2	23	16	57	0
H-1	-7.65	6	3	86	3	0	0	0	2
H-2	-7.79	0	0	0	0	8	61	31	0
H-3	-7.82	0	0	0	0	6	24	69	0
H-4	-7.91	1	6	92	0	0	0	1	0
H-5	-7.96	1	1	1	0	2	3	92	0
H-6	-8.02	2	85	1	0	1	0	1	10
H-7	-8.05	19	54	4	3	9	4	4	3
H-8	-8.11	5	73	2	2	11	6	1	1

H-9	-8.15	16	34	0	5	21	13	6	4
H-10	-8.24	1	89	0	0	5	4	0	0

Table S25. Energies values and percentual group contributions of selected β MO's of complex [Ru^{III}(MeO-bpy)-Ru^V(bda)(O)]³⁺.

MO's (β)	Energy (eV)	Ru _{bda}	bda	DMSO	CN	Ru _{tpy}	tpy	MeO-bpy	O
L+10	-2.69	50	9	10	7	2	0	0	22
L+9	-2.79	1	99	0	0	0	0	0	0
L+8	-2.89	0	2	0	0	3	5	90	0
L+7	-2.91	1	95	0	0	0	1	3	1
L+6	-3.06	0	1	0	0	2	94	3	0
L+5	-3.38	5	72	0	0	1	17	0	5
L+4	-3.41	1	16	0	0	3	78	1	1
L+3	-3.76	57	25	6	6	1	0	0	6
L+2	-4.29	54	25	0	0	0	0	0	21
L+1	-4.79	28	11	4	1	1	0	0	55
LUMO	-5.19	0	0	0	2	73	12	12	1
HOMO	-7.43	1	0	1	3	38	13	43	0
H-1	-7.64	7	3	83	3	3	1	0	1
H-2	-7.8	0	0	0	0	0	75	24	0
H-3	-7.84	2	70	1	0	2	1	2	22
H-4	-7.88	5	14	10	3	16	12	39	1
H-5	-7.9	1	3	37	1	9	10	37	0
H-6	-7.92	1	3	49	3	27	11	6	0
H-7	-8.02	4	8	1	1	6	7	73	0
H-8	-8.08	9	64	4	1	5	4	14	0
H-9	-8.12	11	79	1	1	2	2	4	0
H-10	-8.26	1	98	0	0	0	0	0	1

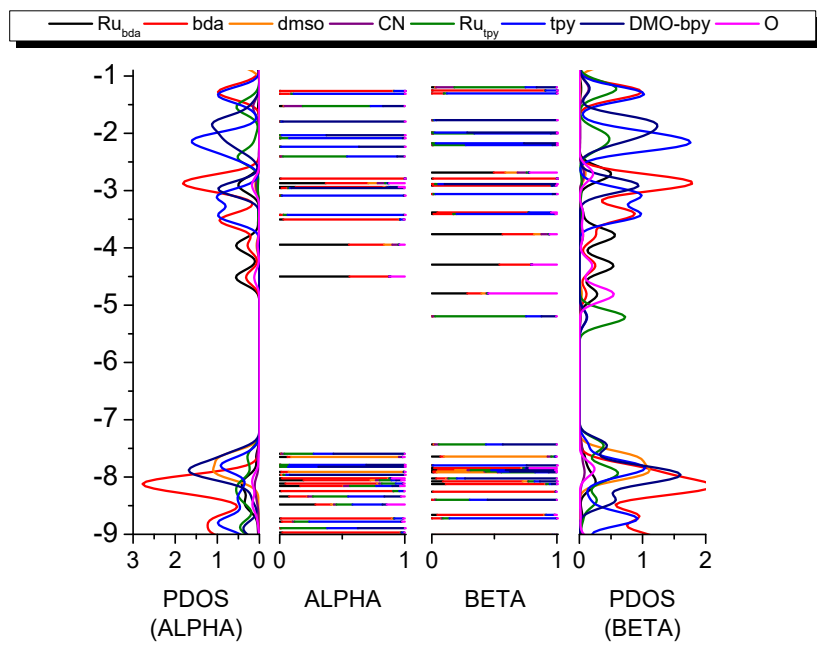


Figure S45. Molecular orbital diagram and partial density of states (PDOS) of complex $[\text{Ru}^{\text{III}}(\text{MeO-bpy})-\text{Ru}^{\text{V}}(\text{bda})(\text{O})]^{3+}$.

Table S26. (TD)DFT assignments for calculated UV-Vis transitions of the complex $[\text{Ru}^{\text{III}}(\text{MeO-bpy})-\text{Ru}^{\text{V}}(\text{bda})(\text{O})]^{3+}$.

No.	Wavelength (nm)	Osc. Strength	Major contributions	Assignment
9	619.5	0.013	H-1(B)->L+1(B) (74%), H-1(B)->LUMO(B) (14%)	$\pi(\text{DMSO}) \rightarrow d(\text{Ru}_{\text{bda}}=\text{O})$
10	601.5	0.018	H-7(B)->LUMO(B) (58%)	$\pi(\text{MeO-bpy}) \rightarrow d(\text{Ru}_{\text{tpy}})$
18	534.8	0.070	H-11(B)->LUMO(B) (63%)	$\pi(\text{MeO-bpy}) \rightarrow d(\text{Ru}_{\text{tpy}})$
53	403.2	0.027	H-1(B)->L+3(B) (30%), H-1(A)->L+1(A) (21%)	$\pi(\text{DMSO}) \rightarrow d(\text{Ru}_{\text{bda}})$
58	397.3	0.024	H-1(B)->L+3(B) (15%), H-22(B)->L+1(B) (14%), H-20(B)->L+1(B) (12%)	$\pi(\text{bda}) \rightarrow d(\text{Ru}_{\text{bda}}=\text{O})$ $\pi(\text{DMSO}) \rightarrow d(\text{Ru}_{\text{bda}}=\text{O})$
135	322.0	0.058	H-3(A)->L+3(A) (28%)	$\pi(\text{MeO-bpy}) \rightarrow \pi^*(\text{tpy})$
149	314.9	0.051	HOMO(A)->L+4(A) (13%), H-15(A)->LUMO(A) (12%), HOMO(B)->L+8(B) (11%)	$d(\text{Ru}_{\text{tpy}}) \rightarrow \pi^*(\text{tpy})$

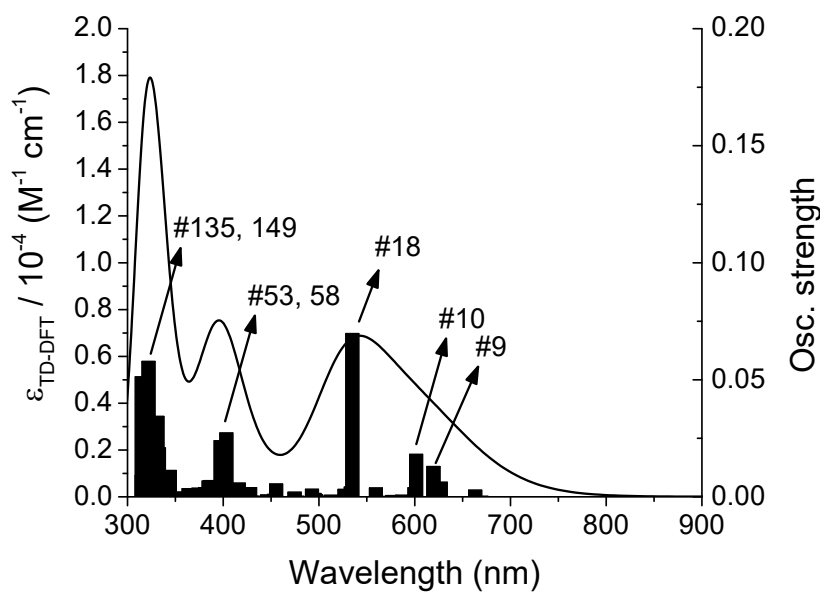


Figure S46. (TD)DFT-calculated UV-visible absorption spectra of complex $[\text{Ru}^{\text{III}}(\text{MeO-bpy})-\text{Ru}^{\text{V}}(\text{bda})(\text{O})]^{3+}$. Calculated transitions are represented by black vertical bars.